Mathematical models of odontogenic cysts and of fractures of jaw-bones. An introductory study

Nedoma, Jiří
2012

Institute of Computer Science
Academy of Sciences of the Czech Republic

Mathematical models of odontogenic cysts and of fractures of jaw-bones

An introductory study

Jiří Nedoma

Technical report No. 1166

June 2012

Pod Vodárenskou věží 2, 182 07 Prague 8, phone: +420 266 051 111, fax: +420 286 585 789,
e-mail:nedoma@cs.cas.cz

Institute of Computer Science
Academy of Sciences of the Czech Republic

Mathematical models of odontogenic cysts and of fractures of jaw-bones

An introductory study

Jiří Nedoma

Technical report No. 1166

June 2012

Abstract:

The mathematical models of quasi-statically loaded odontogenic cysts are formulated and analyzed. Since mechanical loadings, and namely dynamic loadings, play an important role in the development and progression of the jaw-bones with destructive cysts, the analyses of stress-strain fields in the investigated part of the TMJ system can give more information about TMJ joint contact pressures as well as about a crack propagations and about possible fractures of the jaw-bones. The models will be based on the contact problem in nonlinear elastic rheology and/or on the visco-elastic rheology that approximate the jaw-bones. The presented theory and mathematical models can be also used for analyses of cysts situated in long bones or in spine, respectively.

The numerical solutions of the investigated quasi-static problems and corresponding algorithms will be based on the finite element approaches and the contact problems. The algorithms are based on the author's results.

Keywords:
Jaw-bones, TMJ system, long bones, spine, neoplasms, cysts, growth of cyst, osmolality, timely loaded jaw-bones with destructive cysts, linear and nonlinear (thermo-)elasticity, mathematical models, contact problems, jaw-bone fractures, algorithms

1 Introduction

In biology and medical sciences mathematical models play an important role. The role of mathematical models are then to explain a set of biomedical experiments and analyses, and to make certain predictions which will then be tested by further biomedical, biological or numerical experiments as well as further analyses of obtained data. During the last four decades, various neoplasms (cysts, benign and malign tumors) models have been developed, analyzed and discussed. They also need to take into considerations the facts that the tumour regions are changing in time and that their boundaries are unknown in advance and in the literature are known as free boundary problems (e.g. Friedman (1982), (2004)).

By **neoplasm**, or **tumor**, we mean a growing mass of abnormal cells. The neoplasms are distinguished as (i) cysts, (ii) benign tumors and (iii) malign tumors. Cysts are formed either in bones or in soft tissues, respectively. When there are occurred in the bones, they are called central cysts, and when they are occurred in soft tissues they are called peripheral cysts. A special feature in tumor growth is proliferation. Proliferating cells are causes of the tumor volume which varying in time. A tumor contains different populations of cells, such as (i) proliferating cells, i.e. cells that undergo abnormally fast mitosis; (ii) necrotic cells, i.e. cells that died due to a luck of nutrion; (iii) quiescent cells, i.e. cells that are alived but their rate of mitosis is balanced by the rate of natural death.

In growing masses of abnormal cells remain clustered together and confined to the cavity we then speak about **benign tumors**. These types of neoplasms rise relatively slowly, approximately several millimeters per year. In the case that the neoplasms (tumors) have emerged of the cavity, by braking out through the basal membrane and then proliferating into the extracellular matrix, or stroma, then the tumors have been malignant, and we then speak about **malign tumors** or **cancers**. In some cases the cancer cells invade into the blood or the lymphatic vessels and then transported into another locations, where they create secondary tumors. About this process we speak about **metastasis process**. Malign tumors rise relatively very quickly approximately 1mm/day. A primary tumors are traced to mutated cells, from which during short time colonies of cells are formed. In all types of neoplasms a solid tumors can be detected when it reaches a size of several millimeters.

In this study we introduce fundamental ideas how to solve the model problems concerning the analyses of cysts situated in the law-bones and in the long-bones as well as in the spine. Mathematical models for above mentioned types of tumors will be investigated in special studies, while in this study we will introduce the mathematical models of the cysts and methods and algorithms for their solutions only.

2 Odontogenic cysts: definition and their classifications

Cysts are pathological cavity lined by the own epithelium and in the cyst lumen filled by fluid or semi-fluid contents which are not created by the accumulation of pus materials and generally are formed by a connective tissue walls (Figs 1a,b). Odontogenic cysts have epithelial linings which are derived from the epithelial residues of the tooth-forming organs, like rests of Malassez, the reduced enamel epithelium or glands of Serres. The cystic wall is lined by a thin layer of an odontogenic epithelium presenting clear cells and resembling the reduced enamel epithelium. Cysts grow in some cases very slowly, while in the other types (like the keratocysts) they grow relatively quick. During the cyst growth we can assume that the osteolysis is probably rebuilding in the bone tissues, and therefore, the collagen's fibres are connected between the bone tissue and the cyst tissue - the cyst membrane. From the microscopic point of view these transient zones are not sharp, but they changed gradually, and therefore, they can be modelled by thin zones with different material properties. Moreover, in the neighboring bone tissues the properties of bone may be also probably changed in a relatively thin layers from the microscopic point of view in which the osmotic process may be originated.

One of the hypotheses is that inflammation mediators released following the necrosis of the tooth's pulp induces the proliferation and the epithelial rests, while the second one is based on the idea that proliferation of the epithelial avascular tissue may isolate regions of granulation tissue by enclavement of proliferating strands of epithelium about which is assumed that degenerate, we speak about liquefaction necrosis, and create a cavity with increased osmotic potential. Epithelial proliferation

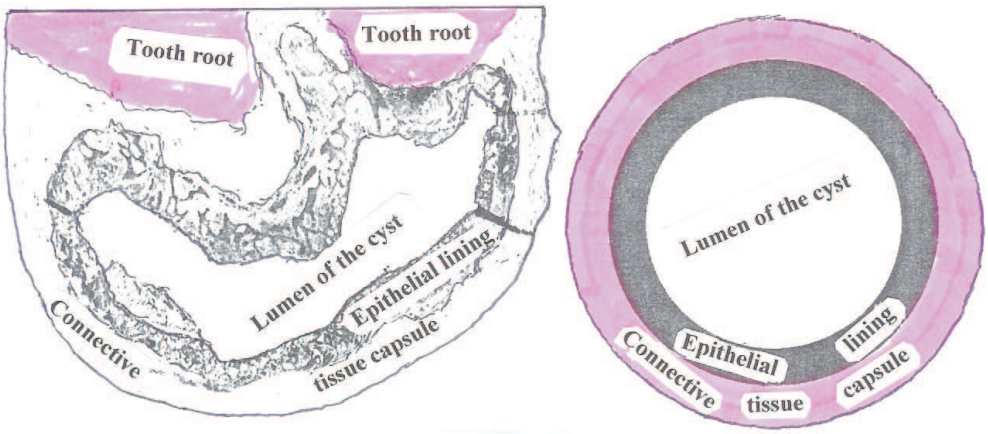

Figure 1: The cysts of (a) prevailing shape, (b) spherical shape.

surrounds the area of necrosis, and therefore, it results the formation of the cysts. In both cases the epithelium is a semi-permeable membrane and the osmotic potential in the cyst cavities lead to an influx of liquids, closed to water, which contribute to increases of hydrostatic pressures of the cysts, and therefore, to their enlargements. The third hypothesis, having well-founded sense in the odontogenic keratocysts observed in jaws of patients with the Gorlin-Goltz syndrome, is assumed on the additional impact that active mitosis of the epithelial cells lining keratocysts have an influence on their rate growths characteristics. The Gorlin-Goltz syndrome is inherited as an autosomal dominant and its main components are nevi and basal cell carcinomas of the facial skin as well as the chest, multiple odontogenic keratocysts and a series of bony abnormalities.

In this study we will limit ourselves to the odontogenic cysts only. **Odontogenic cysts** are cysts of the jaw which are originated (lined) by an odontogenic epithelium (that is, avascular epithelial tissues). They have an epithelial lining which derive from the epithelial residues of the tooth-forming organ - glands of Serres (rests of the dental lamina), rest of Malassez (rest of the root sheath of Hertwig), or the reduced enamel epithelium. **Non-odontogenic cyst**s are those which are originated from other epithelial structures. The odontogenic cysts are divided into two groups - the inflammatory and developmental types. **Inflammatory types** are **radicular (or periapical), residual and paradental cysts**. **Developmental types** are **odontogenic keratocyst or keratocystic odontogenic tumor** (solitary keratocyst or primordial keratocyst and multiple keratocysts, i.e. basal cell nevus syndrome or Gorlin syndrome)**, dentigerous cyst, lateral periodontal cyst, botryoid odontogenic cyst, grandular odontogenic cyst and gingival cyst.** The radicular cysts, the odontogenic keratocysts and the dentigerous cysts are the most important in the stomatological practice, while other types are very rare (Figs 2a–d).

There are several classifications of the odontogenic cysts: WHO classification, Shear's classification and Shaefer's classification.

(I) WHO Classification is divided into two types – development and inflammatory.

- (1) **Developmental cysts**:
  - (a) **Odontogenic cysts:**
    - (i) Primordial (or Kerato) cysts,
    - (ii) Gingival cysts,
    - (iii) Eruption cysts,
    - (iv) Dentigerous (or Follicular) cysts.
  - (b) Non-Odontogenic cysts:

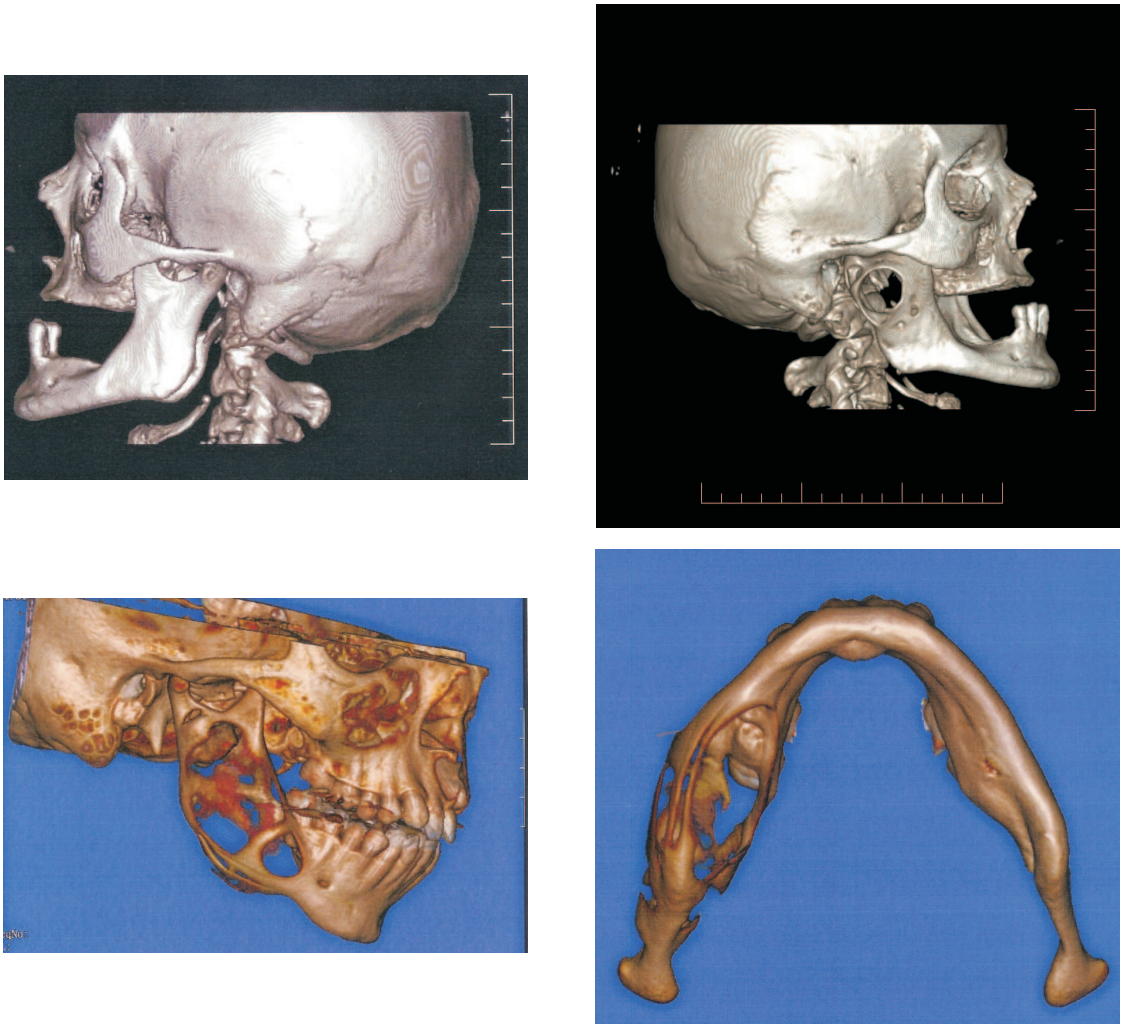

Figure 2: 3D-CT analysis of the TMJ with destructive cysts: (a) the healthy TMJ and the left ramus mandibulae; (b) the destructive cyst in the right ramus mandibulae; (c)–(d) the multiple keratocysts of the TMJ situated in the bone-jaws.

(i) Naso palatine duct (or Incisive canal) cysts,
(ii) Globulomaximillary cysts,
(iii) Naso labial (or Naso alveolar) cysts.

(2) **Inflammatory cysts:**

–
(i) Radicular cysts.

(II) Shear's Classification is divided into third types – cysts of jaw, cysts associated with Maxillary Antrum, cysts of the soft tissues of the Face, Neck and Mouth.

(A) Cysts of Jaw:

•
(1) **Epithelial cysts of jaws:**

–
(α) **Odontogenic cysts:**

(a) **Developmental cysts:**
  (i) Primordial (or Kerato) cysts,
  (ii) Gingival cysts of infants,
  (iii) Gingival cysts of adults,
  (iv) Dentigerous cysts.
  (v) Eruption cysts,
  (vi) Calcifying odontogenic cysts.

(b) **Inflammatory cysts:**
  (i) Radicular cysts,
  (ii) Residual cysts,
  (iii) Inflammatory collateral cysts,
  (iv) Para dental cysts.

(β) **Non-Odontogenic cysts:**
  (i) Naso palatine duct cysts and Incisive canal cysts,
  (ii) Median palatine cysts,
  (iii) Median alveolae cysts,
  (iv) Median mandibular cysts,
  (v) Globulomaximillary cysts,
  (vi) Naso labial (or Naso alveolar) cysts.

(2) **Non-Epithelial cysts of jaws:**

–

(a) **Simple bone cysts:**
  (i) Traumatic cysts,
  (ii) Solitary cysts,
  (iii) Hemorrhagic cysts.

(b) **aneurysmal bone cysts.**

(B) Cysts Associated with the Maxillary Antrum:

•

(1) Benign mucosal cysts,
(2) Surgical ciliated cysts of maxilla.

(C) Cysts of the Soft tissues of the Face, Neck and Mouth:

•

(1) Dermoid and Epidermoid cysts,
(2) Branchial cleft cysts or Lypho epithelial cysts,
(3) Thyroglossal duct cysts,
(4) Anterior median lingual cysts,
(5) Oral cysts with gastro intensional epithelium,
(6) Cystic hygroma,
(7) Cysts of the salivary glands,
(8) Parasitic cysts: Hydatid cysts, Cysticerous cellulosae.

(III) Shaefer's Classification

•

(1) Promordial cysts,

(2) Dentigerous cysts and Eruption cysts,
(3) Periodontal cysts,

–
(i) Apical periodontal cysts;
(ii) Lateral periodontal cysts;

(4) Gingival cysts;

–
(i) Gingival cysts of newborn or Dental lamina cysts,
(ii) Gingival cysts of adult;

(5) Odontogenic Keratocysts

–
(i) Jaw cysts,
(ii) Basal vell nevus and Bifid rib syndrome,

(6) Calcifying odontogenic cysts.

For more details see Killey et al. (1966), Shaefer et al. (1983), Browne (1975), (1990), Fung (1990), Shear (1992), Larsen, Hegtvedt (1998), Shear, Speight (2007), Soames, Southan (1998), Boal (2002), Underbrink and Pou (2002), Goldman (2009).

Since the odontogenic cysts grow within the maxillary bones, they may be causes of bone and tooth resorption, bone fracture, bone expansion or tooth migrations.

The great number of diagnosed odontogenic cysts (OC) are the so-called radicular cysts, i.e., OC associated with the roots of non-vital teeth, which are of about 60–75% of all diagnosed jaw cysts. These cysts arise from the proliferation of the so-called epithelial rests of Malassez (Malassez (1885)). These epithelial rests are the remnants of the root sheath of Hertwig responsible for the formation of the roots of teeth. As it was shown in Ward et al. (2004a,b), Magar et al. (2002) radicular cysts originate from proliferation of epithelial residues (or epithelial rest). These epithelial cells remain quiescent throughout life, however, cell mediators and signalling molecules released during an inflammatory process may trigger their proliferation (Murray (2003), Shear and Speight (2007)).

The mechanisms which take place in the pathogenesis of radicular cysts are described in Magar et al. (2002), Ward et al. (2004a,b) and Shear (1992), etc. and are based on (i) cyst formations and (ii) cyst growth.

(i) **Cyst formation** is based on these ideas: the epithelial proliferation may reach a critical size at which the diffusion of nutrients within the mass of cells cannot keep pace with the metabolic utilization of the nutrients. Owing to the lack of nutrients the central cells in the proliferating mass with subsequent liquefaction degenerate and die and then create a new cavity in the epithelial mass (Figs 3a,b). The products of the epithelial cell degeneration create an osmotic potentials between the interior and exterior of the cysts.
(ii) For the **cyst growth** we assume that the degradation of the central cells in the cyst evokes an increased osmotic pressure in the comparison to the osmotic pressure of stroma surrounding the cyst. This gradient draws fluid [e.g. odontogenic cyst fluids are created by protein, lactoferrin, whose concentration is larger in keratocyst fluids than in dangerous or radicular cyst fluids, but its concentration is not an absolute diagnostic marker for keratocysts (see Toller (1970a,b), Browne (1976), Smith et al. (1983), (1986), Douglas, Craig (1989)); in the simpler theory the cyst fluid can be assumed as the water; the epithelium is a semi-permeable membrana] into the cavity to balance the osmotic pressure, which induces an increase in hydrostatic pressure inside the cyst in comparison to the stroma, and therefore, to its enlargement. The epithelial cells lining the cyst are stimulated to divide at a rate that is consistent with the increase in volume and maintains the width of the epithelial lining. Therefore, the osmotic pressure difference is maintained through the constant shedding of cells into the lumen (due to the fact that the epithelial lining regenerates). The surrounding stroma reorganizes around the cyst wall by producing varying amounts of collagen fibres, the so-called **cystic capsule.** The

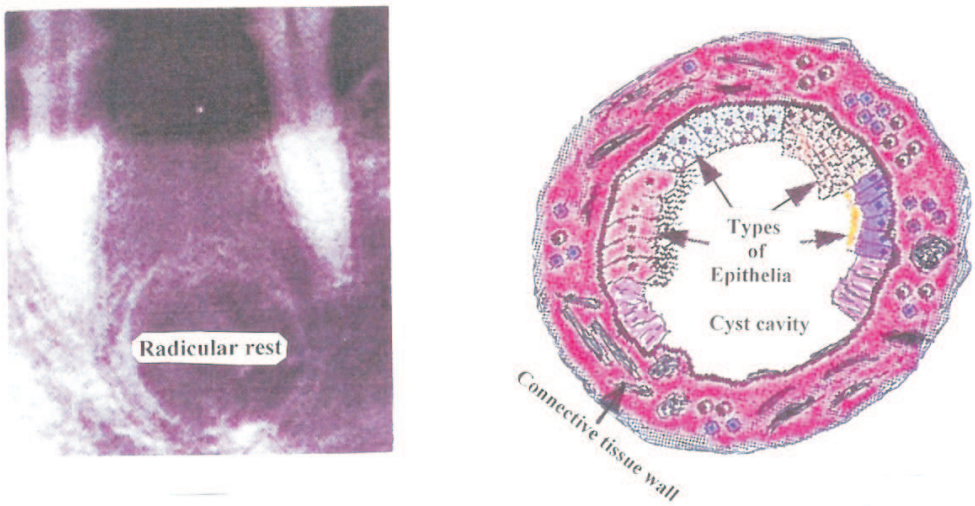

Figure 3: The radicular cyst: (a) location of the radicular cyst, (b) structure of the radicular cyst.

evolution of the odontogenic cyst growth is given in Figs 4a-g. In Fig.4a the odontogenic epithelial rest (OER) in the mandible is situated. Then the cells in the rest (OER) proliferate due to the inflammation (Fig. 4b). The ball of cells growth, the center now starts to be without the nutrion, the central cells die and create a cavity in the epithelial tissue. The center of the ball of cells has a higher protein concentration than the surrounding tissue. Moreover, fluid flows into the central cavity by osmotic pressure and the cyst expands. Around the periphery of the cyst more cells originate while in the center of the cyst more cells die and the protein concentration increases (Figs 4c,d). The osmotic pressure can keep expanding the cyst, at this moment independent of the inflammation so that the cyst further growth (Figs 4e,f), resulting the final state of the radicular cyst at the given time moment (Fig. 4g).

Epithelial cells that line radicular cysts are not malignant, i.e. they do not proliferate unless stimulated by appropriate environmental cues, but the epithelial cells that line another type of odontogenic cyst, the so-called **odontogenic keratocyst**, undergo active mitosis. The process of active division of cells, known as the **mitosis,** is thought to be more important in the growth of keratocysts than in radicular cysts. **Keratocysts** are another type of odontogenic cysts (OC) which have a developmental origin rather than inflammatory (see Shear (1992)). The epithelial lining of these cysts is considered to be form either rests of the lamina (glands of Serres) or extensions of mucosal basal cells. This type of cyst comprise about 5-10% of all diagnosed odontogenic cysts. Keratocysts grow more rapidly than the radicular cysts; they can become extremely large, causing bone resorption and mitotic activity is more commonly observed in their epithelial lining than in vascular cysts. Keratocysts exhibit epithelial budding, i.e. growth into the stromal compartment of the cyst wall, with two consequences: (i) formation of satellite cysts and (ii) a high rate of recurrence after surgery, if the cyst lining is not completely removed. Specific markers for diagnosis of odontogenic keratocysts are pre-albumin, a keratin-like component, and an antigen. Douglas and Craig (1989) reported that lactoferrin seemed to be specific to odontogenic keratocysts. Odontogenic keratocyst fluids contain significantly lower concentration of protein than dentigerous, or radicular/residual cyst fluids. The range of values for keratocyst fluids, however, (0.06–15.8 g/100ml) overlapped those obtained for dentigerous (6.1–17.3 g/100ml) and radicular/residual cyst fluids (2.8–18.0 g/100ml) (Douglas and Craig (1989)).

The tooth cyst can be already originated when the cells, i.e. ameloblasts, sitting on the surface of the tooth enamel of the non-cutting tooth, the so-called **ameloblasts**, continue in their secretional activity created the tooth enamel (encaustum). The tooth cyst grows, the bone becomes weakened resulting the fracture of the jaw-bones (the mandible or the maxilla).

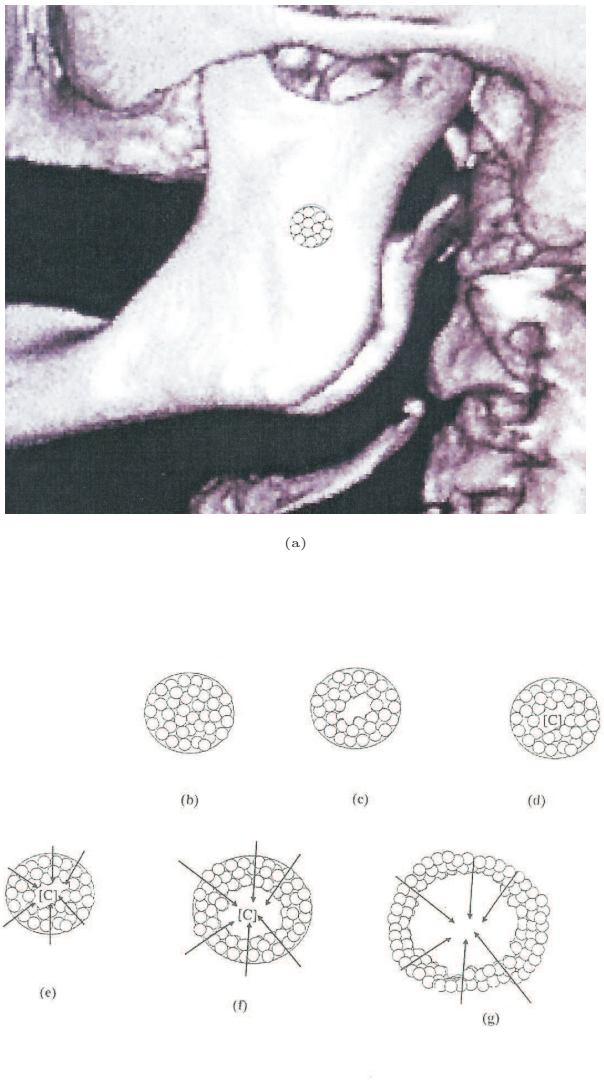

Figure 4: The evolution of odontogenic cyst growth.

3 The jaw-bones with the cysts and analysis of growth of the cyst

In this part of our study we limit ourselves to the mathematical models of cysts only. Since a number of types of cysts, observed in the human body, is relatively high, we will mainly limit ourselves to the odontogenic cysts only. Moreover, most cysts in the human body are functional (benign), but a few of them are tumors or are produced within tumors, and therefore, they can be malignant. Modelling and simulation of tumor growth and stress-strain relationships in the region of the cyst and its neighborhood are certainly of a great interest of applied mathematics which could have an impact both on the quality of patient's life as well as the better understanding of evolution of cyst processes. Odontogenic cysts are in general slow growing and represent in early states of evolution no great problem and treat to human life.

To obtain more information about evolution of the cysts and to find specific conditions for understanding of cyst fundamentals and then for reconstruction of the jaw-bones with cysts besides the knowledge of clinical and radiographic features and specific histologic analyses also analyses of stress-strain distributions in the jaw-bones and determination the possible fractured areas in the jaw-bones are needed. Therefore, mathematical modelling and mathematical simulation of cysts evolutions and

their growth can be useful for better understanding of their fundamentals, their structures and their evolution. The algorithms are based on the author's results (Nedoma (1983), (1987), (1993), (1998), (2005), (2009), (2012), Hlaváček and Nedoma (2002) and Nedoma et al. (1999), (2006), (2011)).

3.1 The model of the cystic growth

Our mathematical model of cystic growth is based on the important diffusive mechanisms, cell birth and death, the idea of osmosis, the balance between osmotic and hydrostatic pressure forces within the cyst structure and its neighborhood. By the **osmosis** we understand the diffusive process of permeability between two different liquids which are mutually separated by a porous membrane.

Osmosis, as a diffusive process, occurs when, to produce equilibrium, a substance in solution crosses a membrane from the region with lower concentration to the region with higher concentration. By **osmolality** we understand that the concentration of particles dissolved in solution expressed as osmoles of solute per kilogram of solvent. The concentration of dissolved particles in the human plasma is $\sim 290 \times 10^{-3}$ M. Therefore, osmolality refers to the number of milliosmoles per kilogram of solvent (Toller (1970b)). Its value can be calculated or can be determined experimentally by osmometry. By **osmolarity** is understood the number of milliosmoles per liter of solution. It is widely used in clinical practice because it expresses concentration as a function of volume. Therefore, osmolarity cannot be measured experimentally, but its value can be determined from osmolality by means of conversion factor. Therefore, due to the concentration $\sim 290 \times 10^{-3}$ M of the human plasma, its osmolarity is 290 mOsm/L. The osmolarity of human plasma is from the interval $285 - 310$ mOsm/L. Water flow from the region of low osmolarity to the region with high osmolarity at a rate directly proportional to the gradient (difference) in osmolality until equilibrium is reached. Solutions containing the same concentrations of particles are iso-osmotic or isotonic (Stranz, Kastango (2002)).

Let us assume that the cyst occupies the region, we denote it by Ω_c (e.g., it can be a sphere of radius R or of an arbitrary shape) with a thin epithelial rim of cells covering its surface. The lumen of the cyst is assumed to be filled by dead cellular material, consisting partly of osmotic material concentration C^+, with total mass S, generating an osmotic pressure. Inside the cyst is observed the hydrostatic pressure, we denote it as P_0^+. The neighborhood of the cyst is created by a material, consisting of a fixed osmotic material of concentration C^-, generating an osmotic pressure P_0^-. The hydrostatic pressure here is P_h^-. According to the size of the cavity the thickness of the capsule and the epithelial layer can be neglected. Throughout development of the cyst its shape is approximately of a spherical form, even when growing into the bony tissue of the jaw. Presumably bone reception is occurring sufficiently fast to accommodate cyst growth. Since radicular cyst growth is slow, the evolution of the radicular cyst may be of several years, while the growth of keratocysts is relatively quick. The growth of radicular cysts is of about a few millimeters per year, while in the keratocysts case their growths are several times higher. Experimental and clinical data show that the mitotic rate is small in radicular cysts, that is, that only a small proportion of living cells are undergoing mitosis at any one time. The osmotic pressure difference $\triangle P_0 = P_0^+ - P_0^-$ relates to the difference in osmolality $\triangle m$, that is,

$$\triangle P_0 = \triangle m R_g T, \tag{3.1}$$

where $\triangle m$ is the molar concentration of "osmotic active" molecular per litre ($\sim$ 0.011 Osml$\equiv$ 0.011 mol), $R_g = 8.31$ J/mol.K is the ideal gas constant, T is the absolute temperature. We see that the osmotic pressure will be dependent on the deformation of the jaw (mandible) as the part of deformation energy change into the heat. Toller (1970b) showed that the osmolality, the molar quantity of "osmotically active" molecules per litre, between cyst fluid and normal tissue fluid, known as serum, is higher in cyst fluid (mean value $\sim$ 0.291 Osml$\equiv$ 0.291 mol) than in serum (mean value $\sim$ 0.280 Osml). These values are consistent across several types of cysts. Thus the osmotic pressure $\triangle P_0$ is ~ 28.3 Nm^{-2}. Therefore, the osmotic process is also slow or relatively quick, but the passage of fluid (fluid passage) through the epithelial membrane in response to the differences between pressures inside the cyst and in its neighborhood is instantaneous. Hence, the hydrostatic pressure difference between the interior of the cyst and the neighborhood balances the osmotic pressure difference between the cyst interior and its neighborhood at the cyst rim, i.e.,

$$P_h^+ - P_h^- = P_0^+ - P_0^-, \tag{3.2}$$

where P_h^+, P_0^+ are the hydrostatic and osmotic pressures, respectively, inside the cyst and P_h^-, P_0^- are the hydrostatic and osmotic pressures, respectively, in its neighborhood.

We assume, that the nutrient sources, as the neighboring local vasculature, are unchangeable through development of the cyst. Therefore, the cyst's epithelial layer keeps a constant mitotic rate. The rates of epithelial birth and death of the cell are balanced approximately to maintain a fixed rim thickness. Since the cyst grows, cells migrate towards the interior of cavity, where they die and since the degraded material driving the osmosis does not penetrate the epithelial layer (i.e. membrane) it then start to be a part of osmotic material. The osmotic material is trapped in the cavity of the cyst and only fluid can pass the semi-permeable epithelial membrane. Assume that "s" is the total amount of degraded material inside the cyst. Then the rate of change of mass of osmotic material in the core in time, i.e., of "$\dot{s} = \frac{ds}{dt}$", is proportional to the surface area of the covering epithelium, we denote it as S_c, then we have

$$\frac{ds}{dt} = \beta S_c, \tag{3.3}$$

where β is a supply rate of the osmotic material, i.e., of degraded material into the cavity, and it can change according to the type of cyst. Its value will be smaller in a cyst which is loosing its cell lining slower than in the case of a radicular cyst, and larger in the case of keratocysts in which the epithelial cells actively divide. Moreover, the parameter β may also comprise the effects of mucous secretions by lining cells which have undergone mucous cell metaplasia. If β increases, the pathological change in the epithelium will increase the amount of osmotically material in the lumen of the cyst. If we assume that the cyst has a spherical shape then $S_c = 4\pi R^2$, where R is a radius of the cyst.

Assume that the concentration of osmotic material is uniform throughout the interior of the cyst. Therefore, the osmotic pressure will be uniform throughout the interior of the cyst. As each epithelial cell contains the same amount of osmotically active substance, then the osmotic pressure is proportional to a concentration of degraded material. The concentration outside the cell is assumed to be constant, hence the osmotic pressure in the neighborhoods is also constant. Therefore, the jump in osmotic pressures across the epithelial lining is proportional to the concentration difference of osmotic material (degraded cells), i.e., it satisfies

$$P_0^+ - P_0^- = \alpha(C^+ - C^-)\,, \tag{3.4}$$

where C^+ is the concentration of material inside the cyst, C^- is the concentration of material outside the cyst, $\alpha = R_g T$ is the proportional coefficient, where R_g is the ideal gas constant, T is the temperature. The Eq. (3.4) is the so-called van Hoff equation (see Tombs, Peacocke (1974)).

The concentration of material inside the cyst is given as its total mass "s" divided by the cavity volume V_c by

$$C^+ = \frac{s}{V_c} = \frac{s}{|\Omega_c|}\,, \tag{3.5}$$

where Ω_c represents the region occupied by the cyst and thus $V_c = |\Omega_c|$. For the spherical cavity of the cyst $V_c = \frac{4}{3}\pi R^3$. This could be valid due to the fact that the growth rate of the cyst is very slow. When the cyst grows into a bony tissue, the bone is resorbed and the cyst grows as there it was no obstacle stopping it from expanding. Therefore, the stresses on the cyst are a little angularly dependent.

The hydrostatic pressure jump across the epithelial membrane balances the stresses in the semi-permeable membrane and the stresses on the cyst (cyst surface) from the neighboring bone tissue (or in general the neighboring tissue, which can be also a soft tissue). Thus

$$P_h^+ - P_h^- = f(\mathbf{r}, \dot{\mathbf{r}}) + f_b(\mathbf{r}, \dot{\mathbf{r}}), \tag{3.6}$$

where f is the **physical stresses,** depending on the material properties of the cyst and the neighboring bone tissue, which is in general a function of a position vector $\mathbf{r}$ of the surface point, and $\dot{\mathbf{r}} = \frac{d\mathbf{r}}{dt}$ the time derivative of $\mathbf{r}$; in the case of an assumed spherical cyst $\mathbf{r} = \mathbf{R}$, where $R = |\mathbf{R}|$ is a radius of the cyst and $\dot{\mathbf{r}} = \dot{\mathbf{R}} = \frac{d\mathbf{R}}{dt}$; and f_b corresponds to the **biological stresses**, i.e., stresses due to biological processes, such as tension shifts in the epithelial lining due to the cell proliferation. These biological stresses may probably play an outstanding role in keratocysts. The natures of these stresses in situ are

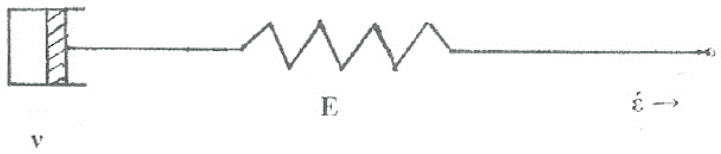

Figure 5: The Maxwell material model.

not known currently and suitable forms can only be estimated. It seems that the contribution to the forces due to biological processes is small in comparison to the physical processes, and therefore, the term $f_b(\mathbf{r},\dot{\mathbf{r}})$ can be omitted, i.e., $f_b(\mathbf{r},\dot{\mathbf{r}}) = 0$. In Magar et al. (2002) the authors also discussed the physical stresses only. They showed that it is not clear which biological or physical stresses would be included. The fact that in some cases the cells actively divide may affect the stresses the surrounding material exerts on the cyst. But it is not clear whether these stresses are important, or whether they are proportional to the rate of change of $\mathbf{r}$, or proportional to the rate of change of the surface area of the cyst.

The material properties of the surrounding material of connective tissue, vasculature and extracellular fluid is clearly complex. Magar et al. (2002) expect that it is mixture of elastic and non-elastic (viscous) materials and that it can be modelled by a linear viscoelastic fluid. Such material behavior is given by the Maxwell model (see Fig. 5). It consists of a linear spring in series with a dashpot. Such model exhibits behavior which are solid-like and fluid-like. The spring models the elastic response with a stiffness E, while the dashpot models the viscous response with a viscosity ν. The total strain is the sum of the elastic and viscous strains

$$\varepsilon = \varepsilon^e + \varepsilon^\nu \,,$$

and the total strain rate is the sum of its elastic and viscous strain rate

$$\dot{\varepsilon} = \dot{\varepsilon}^e + \dot{\varepsilon}^\nu \,,$$

where $\dot{\varepsilon} = \frac{d\varepsilon}{dt}$. Since $\dot{\varepsilon}^e = \frac{\dot{f}}{E}$, and $\dot{\varepsilon}^\nu = \frac{f}{\nu}$, we obtain

$$\dot{f} + \tau^{-1} f = E\dot{\varepsilon} \,, \tag{3.7}$$

where $\tau = \frac{\nu}{E}$ is the so-called **relaxation time**. This means that following a deformation of the stroma, the material will return towards its original shape over the relaxation time τ. E.g. for large τ the material returns close to its original shape, for small τ the material is mostly non-elastic and it maintains roughly its deformed shape.

From (3.4) we find $C^+ - C^- = \frac{1}{\alpha}(P_0^+ - P_0^-)$, i.e., the concentration difference $C^+ - C^-$ is the osmotic pressure difference divided by α. From (3.2) the osmotic pressure difference is equal to the hydrostatic pressure difference, i.e., $\frac{1}{\alpha}(P_0^+ - P_0^-) = \frac{1}{\alpha}(P_h^+ - P_h^-) = \frac{1}{\alpha} f(\mathbf{r},\dot{\mathbf{r}})$ according to (3.6), and therefore, the physical stresses $\frac{1}{\alpha} f(\mathbf{r},\dot{\mathbf{r}}) = C^+ - C^-$. Hence, the concentration of degraded material

$$C^+ = C^- + \frac{1}{\alpha} f(\mathbf{r},\dot{\mathbf{r}}) \,, \tag{3.8}$$

that is, it is a linear function of the stresses, since C^- and α are assumed to be constant.

Since $C^+ = \frac{s}{V_c(\mathbf{r})}$, then substituting $s = C^+ V_c(\mathbf{r})$ into (3.3), i.e., $\frac{ds}{dt} = \beta S_c$, and using (3.8), we obtain

$$\frac{ds}{dt} = \frac{d}{dt}\left[V_c\left(C^- + \frac{1}{\alpha} f(\mathbf{r},\dot{\mathbf{r}})\right)\right] = \beta S_c \,,$$

where β is the core supply rate of osmotic material ([mol/m^2.s]). Hence, performing the differentiation of the product inside the square brackets, we obtain

$$\frac{V_c}{\alpha}\dot{f}(\mathbf{r},\dot{\mathbf{r}}) + \frac{dV_c}{dt}\left(C^- + \frac{1}{\alpha} f(\mathbf{r},\dot{\mathbf{r}})\right)\dot{\mathbf{r}} = \beta S_c \,,$$

hence

$$\frac{\dot{V}_c}{\alpha} f(\mathbf{r},\dot{\mathbf{r}})\dot{\mathbf{r}} + \dot{V}_c C^- \dot{\mathbf{r}} + \frac{V_c}{\alpha}\dot{f}(\mathbf{r},\dot{\mathbf{r}}) = \beta S_c \,. \tag{3.9}$$

representing expression relating the cyst size, its shape and the physical stresses exerted by the stroma.

For the spherical cyst $V_c = \frac{4}{3}\pi R^3$, $S_c = 4\pi R^2$, $\dot{V}_c = 4\pi R^2 \dot{R}$, then (3.9) yields

$$4\pi R^2 \left(C^- + \frac{1}{\alpha} f \right) \dot{R} + \frac{4}{3\alpha}\pi R^3 \dot{f} = 4\pi R^2 \beta \,,$$

hence divided it by $S_c = 4\pi R^2$, we obtain

$$\frac{1}{\alpha} f\dot{R} + C^- \dot{R} + \frac{1}{3\alpha}\dot{f}R = \beta \,. \tag{3.10}$$

Since we model the material which is a mixture of fluid, collagenous capsule, and crystalline structures, and that can be described as a Maxwell fluid, then due to (3.7) the stresses satisfy

$$\tau \dot{f}(\mathbf{r},\dot{\mathbf{r}}) + f(\mathbf{r},\dot{\mathbf{r}}) = \nu\dot{\varepsilon} \,, \tag{3.11}$$

as $\tau = \frac{\nu}{\dot{\varepsilon}}$. For the special case of the spherical cyst, the Eq. (3.11) leads to

$$\tau \dot{f}(R,\dot{R}) + f(R,\dot{R}) = \nu \frac{1}{R}\dot{R} \,, \tag{3.12}$$

where $\dot{\varepsilon} = \frac{1}{R}\frac{dR}{dt}$ is the rate-of-deformation of the spherical cyst. The problem will be complete for its solution, if the initial condition on $\mathbf{r}$ and f will be given. Thus, for $t = 0$

$$\mathbf{r}(0) = \mathbf{r}_0, \quad f(0) = f_0 \,, \tag{3.13}$$

where $\mathbf{r}_0$ and f_0 are given.

For the case of spherical cysts the initial conditions are the following

$$R(0) = R_0, \quad f(0) = f_0 \,, \tag{3.14}$$

where R_0 and f_0 are given. As the model data one can use the following data: $R_0 = 0.0025$ [m], $f_0 = 0.0283$ [Nm^{-2}] and $\alpha = R_g T = 2575$ [Nm/mol], as $R_g \doteq 8.31$ [J/mol.K] and the absolute temperature $T = 310$ [K], $\beta = 2.5 \times 10^{-14}$ [mol/m^2.s] and $\nu = 10^{-2} \div 10^6$ [Nsm^{-2}] is the stroma viscosity and the stroma relaxation time τ is approximately $10^7 - 10^8$ [s]. The value of parameter β was derived under the assumption that an estimated radial growth is of about ~ 2.5mm.yr^{-1}, that is, for the case of radicular cysts. For keratocysts its value is much more greater than for radicular cysts since the epithelial cells are actively divided, and moreover, in this case, the parameter β also describes the effects of mucous secretions by lining cells that have undergone mucous cell metaplasia. (Soames and Southam (1998), Ward et al. (2004)).

Solving Eqs (3.9) and (3.11) with (3.13) we can determine the surface of the cysts that change in time in the case of a prevailing shapes and solving Eqs (3.10) and (3.12) with (3.14) we can determine the surface of the spherical shapes that also change in time, which together with the mathematical description of the timely loaded law-bones with cysts based on the contact mechanics without or with friction represent the model problems with free boundaries. To analyze possible destruction of the timely loaded jaw-bones with destructive cysts the stress-strain analyses in time are necessary to be made. Since the cystic growth are relatively slow, these analyses can be based on the quasi-static contact problems without (or with friction) in linear or nonlinear (thermo-)viscoelasticity coupled with the problem of the cystic growth in time. Such model problems can give us some information about a distribution of stress-strain fields during timely loading jaw-bones with destructive cysts and during the growth of the cysts in time, that is, from their origins up to their clinically observed states.

The problems (3.9), (3.11) with (3.13) and/or (3.10), (3.12) with (3.14) are coupled nonlinear problems in $\mathbf{r}$ and f for the generalized shape of the cyst or in R and f for the spherical shape of the cyst, respectively. These problems are not solvable in terms of regular functions. Therefore, they can be solved numerically or by approximation techniques (see Magar et al. (2002)).

Analysis of the problem for the spherical type of the cysts

To analyze these problems we limit ourselves to the problem (3.10), (3.12), (3.14) in its non-dimensional form, i.e., the variables R, f and t are re-scaled by such a way that all (seven) parameters and all variables are unitless or dimensionless, resulting in a model that the terms are numbers only, while in the initial problem were dimensional quantities (see Ward et al. (2004a,b)).

Setting

$$R = R_0 R^*, \quad f = f_0 f^*, \quad t = \frac{C^- R_0}{\beta} t^*, \tag{3.15}$$

and define

$$\varepsilon^* = \frac{f_0}{\alpha C^-}, \quad \tau^* = \frac{\tau\beta}{C^- R_0}, \quad \nu^* = \frac{\nu\beta}{C^- R_0 f_0}, \tag{3.16}$$

where all quantities with superscript "$*$" are dimensionless. Then the Eqs (3.10) and (3.12) are transformed to the following equations

$$\varepsilon^* f^* \dot{R}^* + \dot{R}^* + \frac{1}{3}\varepsilon^* \dot{f}^* R^* = 1, \tag{3.17}$$

$$\tau^* \dot{f}^* + f^* = \nu^* \frac{\dot{R}^*}{R^*}, \tag{3.18}$$

and the initial conditions

$$R^*(0) = 1, \quad f^*(0) = 1, \tag{3.19}$$

where $\dot{R}^* = \frac{dR^*}{dt}$ and $\dot{f}^* = \frac{df^*}{dt}$.

Since ε^* is small, we can put $\varepsilon^* \doteq 0$, then from (3.17) we find

$$\dot{R}^* \doteq 1, \tag{3.20}$$

hence

$$R^* \simeq t^* + 1. \tag{3.21}$$

Solving (3.18), (3.19), we obtain

$$f^* \simeq e^{-\frac{t^*}{\tau^*}} \left[1 + \frac{\nu^*}{\tau^*} \int_0^{t^*} \frac{e^{\frac{u}{\tau^*}}}{u+1}\, du \right]. \tag{3.22}$$

Since ε^* is small, this fact suggests that when the experimental measurements are taken, the osmotic pressure difference f_0 will have relatively little effect on further cyst development (Ward et al. (2004a,b)). Growth of the cyst is determined by the volume generated by cell birth and by dead cells being deposited in the core. The osmotic pressure can be non-negligible and as it was shown in Ward et al. (2004a,b) it was probably dominate, when R^* is small, that is, $t^* \preceq 0$, that suggests that the cyst originated several years earlier, e.g., if $t^* \sim -t_p^*$, where t_p^* represents the "history" time of the beginning of the cyst growth.

The "cyst history" depends also on the parameters τ^* and ν^* and their values (e.g., $\tau^* \simeq 1$ and $10^{-9} \leq \nu^* \leq 1$).

For large time (e.g. $t^* \geq 3$) then

$$R^* \simeq t^*, \quad f^* \simeq \frac{\nu^*}{\tau^*}. \tag{3.23}$$

In this case that the behavior of the cysts can be predicted for parameter values and not just when ε^* is small as in the previous case, then the detailed analyses can be found in Ward et al. (2004a,b) and Magar et al. (2002).

4 Mathematical models of timely loaded jaw-bones with destructive cysts

4.1 Introduction

The main **bones of facial and skull skeleton** are the following: Frontal and Nasal bones, Zygomatic bone (zygoma), Mandible, Parietal, Temporal, Occipital bones as well as Lacrimal, Spheroid, Ethmoid, Palatine bones, Vomer, etc. Besides the nasal bone, the most fractured bone of the facial skeleton is the zygomatic bone (Norton (2007)). In our next studies, we will limit ourselves to study the existence of the odontogenic cysts situated in the maxilla and the mandible and the possible fractures in the jaw-bones evoked by weakening of the bones due to the existence of the odontogenic cysts.

Mandible is the strongest and largest facial bone, which forms the lower jaw and is divided into five parts, that is, the body, the ramus, which meets the body of the mandible at the angle of the mandible on each side, seceding by the coronoid process, the condylar process and the alveolar process, which extends superiorly from the body and is created by a thick buccal and thin lingual plate of bone. This part of the mandible supports the mandibular teeth. Alveolar bone is resorbed when a tooth is lost. Ramus extends superiorly from the angle of the mandible, where on the medial side of the ramus the mandibular foramen is located. The masseter m. is attached to the lateral side, while the medial pterygoid m. and sphenomandibular lig. are attached to the medial side. Temporalis m. is attached to the coronoid process and the lateral pterygoid muscle is attached to the pterygoid fovea on the neck. The condylar process articulates with the temporal bone in the temporomandibular joint.

Maxilla forms the majority of the skeleton of the face and the upper jaw and it is composed from the body, the frontal process, the zygomatic process, the palatine process and the alveolar process. It articulates with the opposite maxilla and the frontal, sphenoid, nasal, vomer and ethmoid bones, inferior nasal concha, palatine, lacrimal and zygomatic bones and the septal and nasal cartilage. The alveolar process is the part of maxilla that supports all of the maxillary teeth. Alveolar bone is resorbed when a teeth are lost.

The **temporomandibular joint** (TMJ) is a bilaterally shaped joint connecting mandible to temporal bone. The system of both TMJs function bilaterally, any change in this system on one side influents the opposite joint system. TMJ is created from two articulating bone components: (i) the mandibular condyle of ellipsoidal shape with mediolateral diameter of about 20 mm and anteroposterior diameter 10 mm and with the long axis of both condyles about an angle 150–160°, (ii) glenoid fossa of the temporal bone.

Based on the CT or MRI analyses of the jaw-bones, namely the mandible with the cysts, the fractured mandible by using the mathematical models can be simulated and analyzed. The models can be constructed on the basis of boundary value problems and the finite element method for simpler models when we do not assume the existence of movements in the temporomandibular joints or on the contact problems with or without friction and the finite element method both in the linear (thermo-)visco-elasticity or in the nonlinear (thermo-)elasticity when we assume the existence of movements in the temporomandibular joints, and moreover, when we plan to study softening or hardening of bones due to their loading by external forces. Moreover, if we can study fracturing of the jaw-bones, we can apply the h-version or h-p version of finite element methods, which admit to us to determine areas where the deformation energy is accumulated, and therefore, to determine areas with high shear stresses, where the possibility of fracture occurrences are enormous, and moreover, in places where the jaw-bones due to situated cysts are weakened, and therefore, with rather disposition to fractures. But there will be a question whether there exists possibility to strengthening in analogy of the Gothic arch, observed in the hip joint system or not, and/or to hardening of bone-jaw in analogy of hardening of other biomaterials known from the biomechanics. The second question represents the question whether in the studies of the cysts the influence of heat onto the growth of the cysts are observed or not, because these questions are fundamental for our modelling of cysts growth and possibility to fracture the jaw-bones. We saw above that the experimental and clinical data show that the osmotic pressure difference also depends on temperature (see Eq. (3.1)) (Toller (1970b)). Theoretical studies about osmolality indicate that the heat evoked by deformation of the jaw-bones may contribute to the evolution of the cysts.

Since we don't know which kind of conditions may be observed in areas where the shear stresses increase and where the bone tissues may be strengthened (hardened), the non-linear elasticity of a special type can be usefully applied, and in the second case, because the evolution of cysts in the jaw-bones was based on the Maxwell's visco-elastic rheology, the same Maxwell's visco-elastic rheology and/or the thermo-visco-elastic rheology with short memory (Kelvin-Voight) can be used with a great advantage. In all these model problems we can assume that the loading of the jaw-bones, and therefore, also their deformations, are passed over with zero inertia forces, and therefore, they are deformed relatively slowly.

4.2 Construction of model problems

The main principles for construction of models are the following: (i) the geometries of the studied objects must be approximated with attainable high accuracies; (ii) the used rheology, by which we approximate the biomaterials of our studied objects, must correspond to the real biomaterials building the studied objects; (iii) the applied external loading, which are evoked by muscle forces, must satisfy certain conditions which are limited by a tensile strength of acting muscles; (iv) since in many models we limit ourselves to finite bounded domains only, we then determine these domains by such a way, that we specify the domain by applying the useful boundary conditions. The choice of these boundary conditions must be very careful, because by using unsuitable boundary conditions we then compute and then analyze a different model problem that has no direct relation with the studied reality. Frequently the unsuitable choices of boundary conditions are occurred in some approximations represented by using the Dirichlet conditions in places, where the objects or their parts move one together, or in rectifying the curved boundaries by plane surfaces in places, where the curved shapes play, from the biomechanical point of view, an important role, like in the human joints, in the temporomandibular joints, etc. In such cases the movements or shifts are substantially greater than in the real situations, where the shifts are limited by the curved shapes of the joint acetabula. Moreover, the geometries of the studied objects must be the same for the statically and/or for dynaminacally loaded studied objects.

The simplest models that are constructed on the bases of the boundary value problems and the finite element methods, that is, the simpler models, where we do not assume the existence of movements in the temporomandibular joints, are not good models, because such model problems will not approximate well the real situations in the maxilla and the mandible. Mathematical analyses of such types of model problems show that the estimate

$$\|\mathbf{u}\|_1 \leq c\,(\|\mathbf{u}_1\|_1 + \|\mathbf{f}\|_0 + \|\mathbf{P}\|_0)$$

holds, that is, that the solution depends on the boundary conditions as well as the body forces. Therefore, the approximation of the boundary conditions as well as the body forces can influence the solution of the model problem, and therefore, the interpretations of obtained results can not be correct, but in some studied cases they may be absolutely wrong. Therefore, it will be better to study the investigated problems as the contact problems with or without friction, that approximate the reality much more better as the previous type of discussed model problem.

Since we will study the problem of jaw-bones with odontogenic cysts, but with the healthy TMJs, then in the next studies, we will formulate the problem as the contact problem without friction in nonlinear elasticity in the case if we can study the softening and hardening of the bone tissue or in linear thermo-viscoelasticity, for the case if the osmotic pressure difference $\triangle P_0$ depends on the temperature T. Since we saw above that the osmotic pressure is dependent on the deformation of the jaw, and therefore, on a heat, the problem can be also studied in the thermo-viscoelastic rheology or in the nonlinear thermo-viscoelastic rheology. These problems will be studied in next papers.

4.3 The model of jaw-bone with cysts based on the quasi-static contact problem in linear thermo-(visco-)elastic rheology

Let the jaw-bones with cysts occupy a region $\Omega \in \mathbb{R}^N$, $N = 2, 3$. Further, we limit ourselves to the linear thermo-elasticity and the thermo-visco-elasticity with short memory and in more details to the

nonlinear elasticity. We will assume that the inertia term can be omitted.

Let $I = (0, t_p)$ be a time interval. Let $\Omega \subset \mathbb{R}^N$, $N = 2, 3$, be a region occupied by a system of bodies of arbitrary shapes Ω^ι such that $\Omega = \cup_{\iota=1}^r \Omega^\iota$. Let Ω^ι have Lipschitz boundaries $\partial\Omega^\iota$ and let us assume that $\partial\Omega = \Gamma_\tau \cup \Gamma_u \cup \Gamma_c$, where the disjoint parts Γ_τ, Γ_u, Γ_c are open subsets. Moreover, let $\Gamma_{tau} = {}^1\Gamma_{tau} \cup {}^2\Gamma_{tau}$ and $\Gamma_c = \cup_{s,m}\Gamma_c^{sm}$, $\Gamma_c^{sm} = \partial\Omega^s \cap \partial\Omega^m$, $s \neq m$, $s, m \in \{1, \ldots, r\}$, and some of them, we denote them by Γ_0, correspond to the boundaries between the cyst's surfaces and the bone tissues. It is evident that these boundaries are determined by using the algorithm of the cyst's growth. Let $\Omega(t) = I \times \Omega$ denote the time-space domain and let $\Gamma_\tau(t) = \Gamma_\tau \times I$, $\Gamma_u(t) = \Gamma_u \times I$, $\Gamma_c(t) = \Gamma_c \times I$ denote the parts of its boundary $\partial\Omega(t) = \partial\Omega \times I$.

Furthermore, let $\mathbf{n}$ denote the outer normal vector of the boundary, $u_n = u_i n_i$, $\mathbf{u}_t = \mathbf{u} - u_n\mathbf{n}$, $\tau_n = \tau_{ij} n_j n_i$, $\boldsymbol{\tau}_t = \boldsymbol{\tau} - \tau_n\mathbf{n}$ be normal and tangential components of displacement and stress vectors $\mathbf{u} = (u_i)$, $\boldsymbol{\tau} = (\tau_i)$, $\tau_i = \tau_{ij} n_j$, $i, j = 1, \ldots, N$. Let $\mathbf{F}$, $\mathbf{P}$ be the body and surface forces, ρ the density. The respective time derivatives are denoted by "$'$". Let us denote by $\mathbf{u}' = (u_k')$ the velocity vector. Let on Γ_c^{sm} the positive direction of the outer normal vector $\mathbf{n}$ be assumed with respect to Ω^s.

From the momentum conservation law and the entropy density law the equilibrium equation in quasi-static case and the expanded equation of heat conduction are of the form

$$\frac{\partial \tau_{ij}^\iota}{\partial x_j} + f_i^\iota = 0, \quad i, j = 1, \ldots, N,\ \iota = 1, \ldots, r, \quad (\mathbf{x}, t) \in \Omega^\iota(t) = \Omega^\iota \times I\,, \tag{4.1}$$

$$\rho^\iota c_e^\iota \frac{\partial T^\iota}{\partial t} - \rho^\iota \beta_{ij}^\iota T_0^\iota e_{ij}(\mathbf{u}'^\iota) = \frac{\partial}{\partial x_i}\left(\kappa_{ij}^\iota \frac{\partial T^\iota}{\partial x_j}\right) + W^\iota,\ i, j = 1, \ldots, N,\ \iota = 1, \ldots, r,\ (\mathbf{x}, t) \in \Omega^\iota(t) = \Omega^\iota \times I\,, \tag{4.2}$$

where for the linear elastic rheology

$$\begin{aligned} \tau_{ij}^\iota = \tau_{ij}^\iota(\mathbf{u}) &= c_{ijkl}^{(0)\iota}(\mathbf{x}) e_{kl}(\mathbf{u}^\iota) - \beta_{ij}^\iota(\mathbf{x})(T^\iota - T_0^\iota)\,, \\ e_{ij}(\mathbf{u}) &= \frac{1}{2}\left(\frac{\partial u_i}{\partial x_j} + \frac{\partial u_j}{\partial x_i}\right), \quad i, j, k, l = 1, \ldots, N\,,\ \iota = 1, \ldots, r, \end{aligned} \tag{4.3}$$

and for the linear thermo-visco-elastic rheology

$$\begin{aligned} \tau_{ij}^\iota = \tau_{ij}^\iota(\mathbf{u}^\iota, \mathbf{u}'^\iota) &= c_{ijkl}^{(0)\iota}(\mathbf{x}) e_{kl}(\mathbf{u}^\iota) + c_{ijkl}^{(1)\iota}(\mathbf{x}) e_{kl}(\mathbf{u}'^\iota) - \beta_{ij}^\iota(\mathbf{x})(T^\iota - T_0^\iota) = \\ &= {}^e\tau_{ij}^\iota(\mathbf{u}^\iota) + {}^\nu\tau_{ij}^\iota(\mathbf{u}'^\iota) + {}^T\tau_{ij}^\iota(\mathbf{u}^\iota), \quad i, j, k, l = 1, \ldots, N\,,\ \iota = 1, \ldots, r\,, \end{aligned} \tag{4.4}$$

where $c_{ijkl}^{(n)\iota}(\mathbf{x})$, $n = 0, 1$, are anisotropic elastic and viscous coefficients and $e_{ij}(\mathbf{u})$ are components of the small strain tensor, N is the space dimension. For the tensors $c_{ijkl}^{(n)\iota}(\mathbf{x})$, $n = 0, 1$, we assume that they satisfy the symmetric and Lipschitz conditions, that is,

$$\begin{aligned} &c_{ijkl}^{(n)\iota} \in L^\infty(\Omega^\iota), \quad n = 0, 1\,,\ \iota = 1, \ldots, r\,, \\ &c_{ijkl}^{(n)\iota} = c_{jikl}^{(n)\iota} = c_{klij}^{(n)\iota} = c_{ijlk}^{(n)\iota}\,, \\ &c_{ijkl}^{(n)\iota} e_{ij} e_{kl} \geq c_0^{(n)\iota} e_{ij} e_{ij} \quad \forall e_{ij}, \quad e_{ij} = e_{ji} \text{ and a.e. } \mathbf{x} \in \Omega^\iota,\ c_0^{(n)\iota} > 0\,.\ \iota = 1, \ldots, r\,, \end{aligned} \tag{4.5}$$

and the coefficients of thermal conductivity satisfy the symmetric and uniformly definite conditions, that is,

$$\begin{aligned} &\kappa_{ij}^\iota \in L^\infty(\Omega^\iota), \quad \iota = 1, \ldots, r, \quad \kappa_{ij}^\iota = \kappa_{ji}^\iota\,, \\ &\kappa_{ij}^\iota(\mathbf{x}) \xi_i \xi_j \geq \kappa_0^\iota |\xi|^2, \quad \kappa_0^\iota = \text{const } > 0, \quad \forall \xi \in \mathbb{R}^N, \quad \text{and a.e. } \mathbf{x} \in \Omega^\iota \end{aligned} \tag{4.6}$$

and where a repeated index implies summation from 1 to N, the so-called Einstein summation convention. Moreover, $\rho^\iota(\mathbf{x})$ is the density, $c_e^\iota(\mathbf{x})$ is the specific heat, $c^\iota(\mathbf{x}) = \rho^\iota(\mathbf{x}) c_e^\iota(\mathbf{x})$ is the thermal capacity, $\beta_{ij}^\iota(\mathbf{x})$ is the coefficient of thermal expansion, $\mathbf{f}^\iota$ are the body forces, W^ι are the thermal sources.

The problem to be solved has the following classical formulation:

Problem $(\mathcal{P})$: Let $N = 2, 3$, $r \geq 2$. Find a displacement vector $\mathbf{u}^\iota : \overline{\Omega}^\iota \times I \to \mathbb{R}^N$, and a temperature $T^\iota : \overline{\Omega}^\iota \times I \to \mathbb{R}$ satisfying Eqs (4.1) and (4.2) with Eq. (4.3) or (4.4) and the boundary conditions

$$\tau_{ij} n_j = P_i,\ T = T_1, \quad i, j = 1, \ldots, N,\ (\mathbf{x}, t) \in \Gamma_\tau(t) = \cup_{\iota=1}^r (\Gamma_\tau \cap \partial\Omega^\iota) \times I, \tag{4.7}$$

$$u_i = u_{1i},\ T = T_1, \quad i = 1, \ldots, N,\ (\mathbf{x}, t) \in \Gamma_u(t) = \cup_{\iota=1}^r (\Gamma_u \cap \partial\Omega^\iota) \times I, \tag{4.8}$$

$$\left.\begin{array}{l} [u_n]^{sm} \leq 0,\ \tau_n^s = \tau_n^m \equiv \tau_n^{sm} \leq 0,\ [u_n]^{sm} \tau_n^{sm} = 0, \\ \boldsymbol{\tau}_t^{sm} = \mathbf{0}, \\ T^s = T^m,\ \left[\kappa_{ij} \frac{\partial T}{\partial x_j} n_i\right]^{sm} = 0,\ i, j = 1, \ldots, N, \end{array}\right\} (\mathbf{x}, t) \in \cup_{s,m} \Gamma_c^{sm} \times I, \tag{4.9}$$

$$\mathbf{u}^\iota(\mathbf{x}, 0) = \mathbf{u}_0^\iota(\mathbf{x}), \quad T^\iota(\mathbf{x}, 0) = T_0^\iota(\mathbf{x}), \quad \mathbf{x} \in \Omega^\iota, \tag{4.10}$$

where $u_n^s = u_i^s n_i^s$, $u_n^m = u_i^m n_i^s = -u_i^m n_i^m$, $\boldsymbol{\tau}_t^{sm} \equiv \boldsymbol{\tau}_t^s = -\boldsymbol{\tau}_t^m$, and $\mathbf{u}_0$, $\mathbf{u}_1$, T_0, T_1 are given functions, $\mathbf{u}_1$ has a time derivative $\mathbf{u}_1'$, and on $\cup\Gamma_c^{sm}$ due to the equilibrium of forces $\tau_{ij}(\mathbf{u}^s) n_j^s = -\tau_{ij}(\mathbf{u}^m) n_j^m$, $P_i \neq 0$ on ${}^1\Gamma_\tau$, $P_i = 0$ on ${}^2\Gamma_\tau$, $i = 1, ..., N$..

To formulate the problem variationally, we use the following decomposition

$$\mathbf{w}^\iota - \mathbf{u}^\iota = (\mathbf{w}^\iota - \mathbf{u}^\iota + \mathbf{u}'^\iota) - \mathbf{u}'^\iota = \mathbf{v}^\iota - \mathbf{u}'^\iota.$$

Let us introduce the following spaces

$$\begin{aligned} V_0 &= \left\{\mathbf{v} | \mathbf{v} \in \sqcap_{\iota=1}^r H^{1,N}(\Omega^\iota),\ \mathbf{v} = 0 \text{ on } \Gamma_u\right\}, \\ V &= \mathbf{u}_1 + V_0,\ \mathcal{V} = \mathbf{u}_1' + \mathcal{V}_0 = L^2(I; V), \\ \mathcal{K} &= \{\mathbf{v} | \mathbf{v} \in \sqcap_{\iota=1}^s H^{1,N}(\Omega^\iota), \mathbf{v} = \mathbf{u}_1(., t) \text{ on } \Gamma_u,\ [v_n]^{sm} \leq 0 \text{ on } \cup\Gamma_c^{sm}\}, \\ {}^1V_0 &= \left\{z | z \in \sqcap_{\iota=1}^s H^{1,1}(\Omega^\iota), z = 0 \text{ on } \Gamma_u \cup \Gamma_\tau\right\}, \\ {}^1V(t) &= \left\{z | z \in \sqcap_{\iota=1}^s H^{1,1}(\Omega^\iota) \times I, z = T_1(\mathbf{x}, t) \text{ on } \cup_{\iota=1}^r (\Gamma_u \cup \Gamma_\tau) \cap \partial\Omega^\iota\right\}. \end{aligned}$$

Let us assume that $\rho^\iota,\ c_e^\iota \in C\left(\overline{\Omega}^\iota\right),\ \rho^\iota \geq \rho_0^\iota > 0,\ c_e^\iota \geq c_1^\iota > 0,\ \kappa_{ij} \in L^\infty(\Omega^\iota),\ c_{ijkl} \in L^\infty(\Omega^\iota)$, $\beta_{ij} \in C^1(\Omega^\iota)$, $W^\iota \in L^2(I; L^2(\Omega^\iota))$, $\mathbf{f}^\iota \in L^2(I; L^{2,N}(\Omega^\iota))$, $\mathbf{P} \in L^2(I; L^{2,N}(\Gamma_\tau))$, $\mathbf{u}_0^\iota \in H^{1,N}(\Omega^\iota)$, $\mathbf{u}_1^\iota \in L^2(I; H^{1,N}(\Omega^\iota))$, $T_1^\iota \in L^2(I; H^{1,1}(\Omega^\iota))$, $T_0^\iota \in H^{1,1}(\Omega^\iota)$.

Then multiplying (4.1) by $\mathbf{v} - \mathbf{u}'$, where $\mathbf{v}$ are suitable test functions satisfying the above decomposition and (4.2) by $z - T$, where z are suitable test functions, integrating over $\Omega^\iota \times I$, for all ι, using the Green's theorems and boundary and contact conditions, then we obtain the following variational problem:

Problem $(\mathcal{P})_v$: Find a pair of functions $(\mathbf{u}, T)$, $\mathbf{u}(., t) \in \mathcal{K}(t)$ for a.e. $t \in I$, $T(., t) \in {}^1V(t)$ for a.e. $t \in I$ and every $\mathbf{w}(t) \in \mathcal{K}(t)$, $z(t) \in {}^1V(t)$ such that

$$A(\mathbf{u}, \mathbf{u}', \mathbf{v} - \mathbf{u}') + b_s(T - T_0, \mathbf{v} - \mathbf{u}') \geq (\mathbf{f}, \mathbf{v} - \mathbf{u}') \tag{4.11}$$

$$(T', z - T) + a_T(T, z - T) + b_p(\mathbf{u}, z - T) \geq (W, z - T) \tag{4.12}$$

hold, where we assume that the initial data $\mathbf{u}_0$, T_0 satisfies, e.g., the static contact multibody linear

thermo-elastic problem (Nedoma (1987)), and where

$$A(\mathbf{u},\mathbf{u}',\mathbf{w}) = \sum_{\iota=1}^{r} A^{\iota}(\mathbf{u}^{\iota},\mathbf{u}'^{\iota},\mathbf{w}^{\iota}) = \int_{\Omega} \tau_{ij}(\mathbf{u},\mathbf{u}')e_{ij}(\mathbf{w})d\mathbf{x}$$

for the linear viscoelastic rheology,

$$A(\mathbf{u},\mathbf{w}) = \sum_{\iota=1}^{r} A^{\iota}(\mathbf{u}^{\iota},\mathbf{w}^{\iota}) = \int_{\Omega} \tau_{ij}(\mathbf{u})e_{ij}(\mathbf{w})d\mathbf{x}$$

for the linear elastic rheology,

$$(\mathbf{F},\mathbf{w}) = \sum_{\iota=1}^{r} (\mathbf{F}^{\iota},\mathbf{w}^{\iota}) = \int_{\Omega} \mathbf{f}\cdot\mathbf{w}d\mathbf{x} + \int_{\Gamma_{\tau}} \mathbf{P}\cdot\mathbf{w}ds,$$

$$b_s(T,\mathbf{w}) = \sum_{\iota=1}^{r} b_s^{\iota}(T^{\iota},\mathbf{w}^{\iota}) = \int_{\Omega} \frac{\partial}{\partial x_j}(\beta_{ij}T)w_i d\mathbf{x},$$

$$(T',z) = \sum_{\iota=1}^{r} (T'^{\iota},z^{\iota}) = \int_{\Omega} \rho c_e T' z d\mathbf{x},$$

$$a_T(T,z) = \sum_{\iota=1}^{r} a_T(T^{\iota},z^{\iota}) = \int_{\Omega} \kappa_{ij}\frac{\partial T}{\partial x_j}\frac{\partial z}{\partial x_i}d\mathbf{x},$$

$$b_p(w,z) = \sum_{\iota=1}^{r} b_p^{\iota}(w^{\iota},z^{\iota}) = \int_{\Omega} \rho T_0\beta_{ij}\frac{\partial w_i}{\partial x_j}z d\mathbf{x},$$

$$(W,z) = \sum_{\iota=1}^{r} (W^{\iota},z^{\iota}) = \int_{\Omega} W z d\mathbf{x}.$$

Since $\beta_{ij}^{\iota} \in C^1(\Omega^{\iota})$, $T^{\iota}, T_0^{\iota} \in H^{1,1}(\Omega^{\iota})$, then $\beta_{ij}^{\iota}(T^{\iota} - T_0^{\iota}) \in H^{1,1}(\Omega^{\iota})$, and therefore, $\frac{\partial}{\partial x_j}(\beta_{ij}^{\iota}(T^{\iota} - T_0^{\iota})) \in L^2(\Omega^{\iota})$. The bilinear forms $a^{(n)\iota}(\mathbf{u}^{\iota},\mathbf{w}^{\iota})$, $n = 0,1$, are symmetric in $\mathbf{u}^{\iota}$, $\mathbf{w}^{\iota}$ and satisfy $a^{(n)\iota}(\mathbf{u}^{\iota},\mathbf{u}^{\iota}) \geq c_0^{(n)\iota}\|\mathbf{u}^{\iota}\|_{1,N}^2$, $c_0^{(n)\iota} = \text{const.} > 0$, $\left|a^{(n)\iota}(\mathbf{u}^{\iota},\mathbf{w}^{\iota})\right| \leq c_1^{(n)\iota}\|\mathbf{u}^{\iota}\|_{1,N}\|\mathbf{w}^{\iota}\|_{1,N}$, $c_1^{(n)\iota} = \text{const.} > 0$, $\mathbf{u}^{\iota},\mathbf{w}^{\iota} \in H^{1,N}(\Omega^{\iota})$ and the bilinear form $a_T^{\iota}(T^{\iota},z^{\iota})$ is symmetric in T^{ι}, z^{ι} and satisfy $a_T^{\iota}(T^{\iota},T^{\iota}) \geq a_0^{\iota}\|T^{\iota}\|_{1,1}^2$, $a_0^{\iota} = \text{const} > 0$, $|a_T^{\iota}(T^{\iota},z^{\iota})| \leq a_1^{\iota}\|T^{\iota}\|_{1,1}\|z^{\iota}\|_{1,1}$, $a_1^{\iota} = \text{const} > 0$.

The existence of the solution of such problem is parallel to that of Andersson (2000) and Eck et al. (2005). The numerical solution of the problem is based on the finite element techniques and the PDAS algorithm, which will be discussed in more details in the next papers concerning the loaded spine, long bones and the jaw-bones with tumors. This algorithm is discussed in Nedoma (2005), (2010), (2012), Nedoma et al. (2011). The other algorithms are discussed in Nedoma (1998), Nedoma et al. (2011).

4.4 The model of jaw-bone with cysts based on the quasi-static contact problem in nonlinear elasticity

Let the jaw-bones with cysts occupy a region $\Omega \subset R^N$, $N = 2,3$ as above, where a region Ω is occupied by a system of elastic bodies Ω^{ι}, such that $\Omega = \cup_{\iota=1}^{r}\Omega^{\iota}$. Let Ω^{ι} be bounded domains with Lipschitz boundaries $\partial\Omega^{\iota}$. Let us assume that $\partial\Omega = \cup_{\iota=1}^{r}\partial\Omega^{\iota} = \Gamma_u \cup \Gamma_{\tau} \cup \Gamma_c\,(\cup\Gamma_0)$, where Γ_u, Γ_{τ}, Γ_c are open subsets of $\partial\Omega$, and where Γ_u denotes the part of boundary where the studied part of the jaw-bones are fixed, Γ_{τ} denotes the part of boundary where the studied part of jaw-bones are loaded or unloaded, respectively, and $\Gamma_c \neq \emptyset$, $\Gamma_c = \cup_{s,m}\Gamma_c^{sm}$, represents the contact boundary between components of the temporomandibular joints, or e.g., between different parts of the fractured jaw-bone and Γ_0 represents the boundary between the cysts and the bone tissues. Since on the boundary between the cyst and the neighboring bone tissue the normal displacements and normal stresses are equal to zero, therefore, it can be described by the bilateral condition. By indices s, m we denote the neighboring components of the TMJ or fractured parts of the jaw bones. Let $\overline{I} = [0,t_p]$, $t_p > 0$, be the time interval. Let

$\Omega(t) = \Omega \times I$ denote the time-space region occupied by the jaw-bones in time and let $\Gamma_\tau(t) = \Gamma_\tau \times I$, $\Gamma_u(t) = \Gamma_u \times I$, $\Gamma_c(t) = \Gamma_c \times I$, denote the parts of its boundary $\partial\Omega(t) = \partial\Omega \times I$.

Let us assume that the rheology of the jaw-bones can be described by a non-linear stress-strain relation as follows:

Let the deformation energy W be the nonlinear function of strain defined by (see Fung (1965), (1968), (1990), (1993), Nedoma and Hlaváček (2002), Nedoma et al. (2010))

$$W = A^\lambda(e_{ij}) = (c_{ijkl}(\mathbf{x})e_{ij}(\mathbf{u})e_{kl}(\mathbf{u}))^\lambda, \quad A(e_{ij}) = c_{ijkl}(\mathbf{x})e_{ij}(\mathbf{u})e_{kl}(\mathbf{u})\,, \tag{4.13}$$

where $c_{ijkl}(\mathbf{x}) \in L^\infty(\Omega)$ are anisotropic elastic coefficients in linear elasticity satisfying the well-known symmetry and Lipschitz conditions and λ is a parameter. Then

$$\tau_{ij} = \frac{\partial W}{\partial e_{ij}} = 2\lambda A^{\lambda-1}(e_{ij})c_{ijkl}(\mathbf{x})e_{kl}(\mathbf{u}) = c^*_{ijkl}(\mathbf{u})e_{kl}(\mathbf{u}), \tag{4.14}$$

where $c^*_{ijkl}(\mathbf{u})$ are anisotropic nonlinear elastic coefficients satisfying also the symmetry and Lipschitz conditions, that is,

$$\begin{aligned} &c^*_{ijkl}(\mathbf{u}) = c^*_{jikl}(\mathbf{u}) = c^*_{klij}(\mathbf{u}) = c^*_{ijlk}(\mathbf{u}), \\ &c^*_{ijkl}(\mathbf{u})e_{ij}(\mathbf{u})e_{kl}(\mathbf{u}) \geq c^*_0 e_{ij}(\mathbf{u})e_{ij}(\mathbf{u}), \quad \forall e_{ij}, \quad c_0 > 0,\ e_{ij}(\mathbf{u}) = e_{ji}(\mathbf{u}) \quad \text{for a.e. } \mathbf{x} \in \Omega\,. \end{aligned} \tag{4.15}$$

Hence for $0 < \lambda < 1$ the biomaterial is soften, for $\lambda = 1$ is elastic and for $\lambda > 1$ is hardened. In the following we will assume that a repeated index implies summation over the range $1, \ldots, N$. Let us denote by

$$e_{ij}(\mathbf{u}) = \frac{1}{2}\left(\frac{\partial u_i}{\partial x_j} + \frac{\partial u_j}{\partial x_i}\right), \quad i,j = 1,\ldots,N, \tag{4.16}$$

the small strain tensor, $\mathbf{u} = (u_i)$ is the displacement vector. Let $u_n = u_i n_i$, $\mathbf{u}_t = \mathbf{u} - u_n\mathbf{n}$, $\tau_n = \tau_{ij}n_j n_i$, $\boldsymbol{\tau}_t = \boldsymbol{\tau} - \tau_n\mathbf{n}$ are normal and tangential components of displacement and stress vectors $\mathbf{u} = (u_i)$, $\boldsymbol{\tau} = (\tau_i)$, $\tau_i = \tau_{ij}n_j$, $i,j = 1,\ldots,N$, $\mathbf{n} = (n_i)$ is the unit outward normal vector to $\partial\Omega$. Since in the investigated cases of the jaw-bones with cysts we will assume the healthy temporomandibular joints, therefore, we will assume that the friction in the TMJ can be neglected. Such problems lead to the model problems without friction. Finally, let the body forces $\mathbf{f} \in L^2(I; L^{2,N}(\Omega))$ and surface forces $\mathbf{P} \in L^2(I; L^{2,N}(\Gamma_\tau))$. Then we have the following model problem to be solved:

Problem ($\mathcal{P}$): Let $N = 2, 3$, $r \geq 2$. Find a vector function $\mathbf{u} : \overline{\Omega} \times I \to \mathbb{R}$ satisfying

$$\frac{\partial \tau^\iota_{ij}(\mathbf{u}(t))}{\partial x_j} + f^\iota_i(t) = 0, \quad i,j = 1,\ldots,N,\ \iota = 1,\ldots,r,\ (\mathbf{x},t) \in \Omega^\iota(t) = \Omega^\iota \times I\,, \tag{4.17}$$

$$\tau_{ij} = c^*_{ijkl}(\mathbf{u})e_{kl}(\mathbf{u}), \quad i,j,k,l = 1,\ldots,N,\ \iota = 1,\ldots,r, \tag{4.18}$$

$$\mathbf{u} = \mathbf{u}_1(=\mathbf{0}), \quad i = 1,\ldots,N,\ (\mathbf{x},t) \in \Gamma_u(t) = \cup_{\iota=1}^r\,(\Gamma_u \cap \partial\Omega^\iota)\,, \tag{4.19}$$

$$\tau_{ij}n_j = P_i \quad i,j = 1,\ldots,N,\ (\mathbf{x},t) \in \Gamma_\tau(t) = \cup_{\iota=1}^r\,(\Gamma_\tau \cap \partial\Omega^\iota) \times I\,, \tag{4.20}$$

$$\begin{aligned} &[u_n]^{sm} \leq 0, \quad \tau_n^{sm} \leq 0, \quad [u]^{sm}\tau_n^{sm} = 0, \\ &\boldsymbol{\tau}_t^{sm} = \mathbf{0} \end{aligned} \qquad (\mathbf{x},t) \in \Gamma_c^{sm}(t) = \Gamma_c^{sm} \times I\,, \tag{4.21}$$

$$\mathbf{u}(\mathbf{x},t) = \mathbf{u}_0(\mathbf{x})(\equiv \mathbf{0}) \quad \mathbf{x} \in \Omega = \cup_{\iota=1}^r \Omega^\iota, \tag{4.22}$$

where $[u_n]^{sm} = u_n^s - u_n^m$, $[\mathbf{u}_t]^{sm} = \mathbf{u}_t^s - \mathbf{u}_t^m$, and $\tau_n^{sm} \equiv \tau_n^s = \tau_n^m$, $\boldsymbol{\tau}_t^s = -\boldsymbol{\tau}_t^m \equiv \boldsymbol{\tau}_t^{sm}$, and moreover, where $\mathbf{u}_0(\mathbf{x})$ is a given function, e.g. the solution of the static contact problem representing the initial state corresponding to the initial stress-strain distribution in the jaw-bones with cysts in the initial state of cyst′s evolution.

Weak solution of the problem

Let us introduce the following sets

$$V_0 = \{\mathbf{v} | \mathbf{v} \in \sqcap_{\iota=1}^{r} H^{1,N}(\Omega^\iota),\ \mathbf{v} = 0 \text{ on } \Gamma_u\} \quad \text{and} \quad \mathcal{V} = \mathbf{u}_1' + V_0,$$
$$\mathcal{K}(t) = \left\{\mathbf{v} | \mathbf{v} \in \sqcap_{\iota=1}^{r} H^{1,N}(\Omega^\iota),\ \mathbf{v} = \mathbf{u}_1(t,.) \text{ on } \Gamma_u \text{ and } [v_n]^{sm} \leq 0 \text{ on } \cup_{s,m} \Gamma_c^{sm}\right\}.$$

Multiplying (4.17) by $v_i - u_i$, integrating over Ω and using the Green theorem and boundary conditions, we obtain the following variational inequality problem:

Problem $(\mathcal{P})_v$: Find a function $\mathbf{u}(t,.) \in \mathcal{K}(t)$ for a.e. $t \in I$ such that for a.e. $t \in I$ and every $\mathbf{v} \in \mathcal{K}(t)$

$$a(\mathbf{u}; \mathbf{u}, \mathbf{v} - \mathbf{u}) \geq (\mathbf{F}, \mathbf{v} - \mathbf{u}) \tag{4.23}$$

holds, where

$$\begin{aligned} a(\mathbf{w}; \mathbf{u}, \mathbf{v}) &= \int_\Omega \tau_{ij}(\mathbf{u}) e_{ij}(\mathbf{v}) d\mathbf{x} = \\ &= \int_\Omega 2\lambda A^{\lambda-1}(e_{ij}(\mathbf{w})) c_{ijkl}(\mathbf{w}) e_{ij}(\mathbf{u}) e_{kl}(\mathbf{v}) d\mathbf{x} = \int_\Omega c_{ijkl}^*(\mathbf{w}) e_{ij}(\mathbf{u}) e_{kl}(\mathbf{v}) d\mathbf{x}, \end{aligned} \tag{4.24}$$

$$(\mathbf{F}, \mathbf{v}) = \int_{\Gamma_\tau} P_i u_i ds + \int_\Omega f_i v_i d\mathbf{x}. \tag{4.25}$$

To prove the existence of the problem the secant modulus method and the results of Andersson (2000) can be used.

Next, we introduce **the secant-modulus (Kachanov) method for variational inequalities**. Firstly, let us introduce the following assumptions:

Assumptions:

(i) Let K be a nonempty closed convex set in the real Hilbert space V, let $b \in V'$ and let $u_0 \in K$ be given.

(ii) The functional $L : K \to \mathbb{R}$ is G-differentiable. There exists a functional $B : K \times V \times V \to \mathbb{R}$ such that, for $u, v, w \in K$, we have the representation formula

$$\langle L'(u), v - w \rangle = B(u; u, v - w) \tag{4.26}$$

and the key inequality

$$L(v) - L(u) \leq 2^{-1} \left(B(u; v, v) - B(u; u, u)\right). \tag{4.27}$$

(iii) For each $u \in K$, the map $(v, w) \mapsto B(u; v, w)$ is bilinear, bounded, and symmetric from $V \times V$ to $\mathbb{R}$. There exist numbers $\rho > 0$ and $\delta > 0$ such that

$$|B(u; v, w)| \leq \delta \|v\| \, \|w\| \quad \text{for all } u \in K, v, w \in V$$

and

$$B(u; w - v, w - v) \geq \rho \|w - v\|^2 \quad \text{for all } u, v, w \in K.$$

(iv) The operator $L' : K \to V'$ is continuous and strongly monotone, i.e., there is a number $\rho_0 > 0$ such that

$$\langle L'(u) - L'(v), u - v \rangle \geq \rho_0 \|u - v\|^2 \quad \text{for all } u, v \in K.$$

Theorem 1 *Let (i)–(iii) hold. Let $j : V \to \mathbb{R}$ be weakly lower semi-continuous,*

$$j(v) \geq 0 \quad \forall v \in V \quad \textit{and} \quad |j(u) - j(v)| \leq C\|u - v\| \quad \forall u, v \in V.$$

Then: (a) for $k = 0, 1, \ldots,$ the quadratic variational problem

$$2^{-1}B(u_k; u_{k+1}, u_{k+1}) - b(u_{k+1}) = \min! \ , \ u_{k+1} \in K, \tag{4.28}$$

has a unique solution u_{k+1}, and

$$B(u_k; u_{k+1}, v - u_{k+1}) - j(v) - j(u_{k+1}) \geq b(v - u_{k+1}) \quad \textit{for all}; v \in K. \tag{4.29}$$

(b) If, in addition, (iv) holds, then the original variational problem

$$L(u) - b(u) = \min! \quad u \in K,$$

has a unique solution u. Moreover, u is the unique solution of the variational inequality

$$\langle L'(u), v - u\rangle + j(v) - j(u) \geq b(v - u) \quad \textit{for all } v \in K \quad \textit{and fixed } u \in K, \tag{4.30}$$

and the secant modules method converges, that is

$$u_k \to u \quad \textit{in } V \textit{ as } k \to \infty.$$

For the proof see Han, Jensen, Shimansky (1997); for $j \equiv 0$ see Zeidler (1990).

To analyze our model problem, we introduce the following assumptions:

Presumption 1 *Let $N = 3$ and let $\Omega = \cup_{\iota=1}^{r}\Omega^{\iota}$ be a bounded and connected set with Lipschitz boundary $\partial\Omega = \Gamma_\tau \cup \Gamma_u \cup \Gamma_c$, where the disjoint parts $\Gamma_\tau, \Gamma_u, \Gamma_c$ are open subsets. Let $\Gamma_\tau = {}^1\Gamma_\tau \cup {}^2\Gamma_\tau$ and $\Gamma_c = \cup_{s,m}\Gamma_c^{sm}$, $\Gamma_c^{sm} = \partial\Omega^s \cap \partial\Omega^m, s \neq m, \ s, m \in \{1, \ldots, r\}$. Let $\Omega(t) = \Omega \times I$ denote the time-space domain and let $\Gamma_\tau(t) = \Gamma_\tau \times I$, $\Gamma_u(t) = \Gamma_u \times I$, $\Gamma_c(t) = \Gamma_c \times I$ denote the parts of its boundary $\partial\Omega(t) = \partial\Omega \times I$. The coefficients $c^*_{ijkl}(\mathbf{x}, \mathbf{u})$ satisfy (4.15). The given input data satisfy $\rho \in C(\Omega)$, $\mathbf{F}, \mathbf{F}' \in L^2\left(I; L^{2,N}(\Omega)\right)$, $\mathbf{P}, \mathbf{P}' \in L^2(I; L^{2,N}(\Gamma_\tau))$, $\mathbf{u}_1 \in H^{1,N}(\Omega)$, $u^s_{1n} - u^m_{1n} = 0$ on $\cup_{s,m}\Gamma_c^{sm}, \mathbf{u}_0 \in H^{1,N}(\Omega)$. Let M be an integer, then $k = t_p/M$ is a time step.*

Let us introduce the set of virtual displacements and the set of admissible displacements by

$$\begin{aligned} V_0 &= \{\mathbf{v} \mid \mathbf{v} \in H^{1,N}(\Omega^1) \times \cdots \times H^{1,N}(\Omega^r), \mathbf{v} = 0 \text{ on } \cup_{\iota=1}^{r}\left(\Gamma_u \cap \partial\Omega^{\iota}\right), [v_n]^{sm} = 0 \text{ a.e. on } \cup_{s,m}\Gamma_c^{sm}\}, \\ V &= \mathbf{u}_2 + V_0, \\ K &= \{\mathbf{v} \mid \mathbf{v} \in V, [v_n]^{sm} \leq 0 \quad \text{a.e. on } \cup_{s,m}\Gamma_c^{sm}\}. \end{aligned}$$

We multiply the equation (4.17) by $\mathbf{v} - \mathbf{u}$, where $\mathbf{v}$ are suitable test functions, integrating over $\Omega \times I$, using the Green's theorem and boundary conditions, then we obtain the following variational problem:

Problem $(\mathcal{P})_v$: Find a displacement field $\mathbf{u} : \overline{I} \to V$ such that $\mathbf{u}(t) \in K$ for a.e. $t \in I$, and

$$\int_I a\left(\mathbf{u}(t); \mathbf{u}(t), \mathbf{v} - \mathbf{u}(t)\right) dt \geq \int_I (\mathbf{f}(t), \mathbf{v} - \mathbf{u}(t))dt \quad \forall \mathbf{v} \in K, \quad \text{a.e. } t \in I, \tag{4.31}$$

$$\mathbf{u}(\mathbf{x},0) = \mathbf{u}_0(\mathbf{x}), \quad \mathbf{x} \in \Omega, \tag{4.32}$$

where we assume that the initial data $\mathbf{u}_0$ are the given data, e.g., they can be determined as a solution of the following static problems in linear or nonlinear elasticity (e.g., for the linear case see Nedoma (1983), (1987) and Nedoma, Hlaváček (2002) for the nonlinear case):

$$\begin{aligned} &\mathbf{u} \in K, \\ &a(\mathbf{u}, \mathbf{v} - \mathbf{u}, \mathbf{v} - \mathbf{u}) \quad \forall \mathbf{v} \in K, \end{aligned} \tag{4.33}$$

$$a(\mathbf{w};\mathbf{u},\mathbf{v}) = \sum_{\iota=1}^{r} a^{\iota}(\mathbf{w}^{\iota};\mathbf{u}^{\iota},\mathbf{v}^{\iota}) = \int_{\Omega} c^{*}_{ijkl}(\mathbf{w}) e_{kl}(\mathbf{u}) e_{ij}(\mathbf{v}) d\mathbf{x},$$

$$(\mathbf{f},\mathbf{v}) = \sum_{\iota=1}^{r} (\mathbf{f}^{\iota},\mathbf{v}^{\iota}) = \int_{\Omega} F_i v_i d\mathbf{x} + \int_{\Gamma_\tau} P_i v_i ds,$$

where the bilinear form $a(\mathbf{w};\mathbf{u},\mathbf{v})$ is symmetric in $\mathbf{u},\mathbf{v}$ and satisfies $a(\mathbf{w};\mathbf{u},\mathbf{v}) \geq c_0^{*}\|\mathbf{u}\|^2_{1,N}$, $c_0^{*} =$ const. > 0, $|a(\mathbf{w};\mathbf{u},\mathbf{v})| \leq c_1^{*}\|\mathbf{u}\|_{1,N}\|\mathbf{v}\|_{1,N}$, $c_1^{*} =$ const. > 0, $\mathbf{u},\mathbf{v} \in V$.

Numerical solution

Let the $3D$ domain Ω be approximated by Ω_h, being a polyhedron, with the boundary $\partial\Omega_h = \Gamma_{\tau h} \cup \Gamma_{uh} \cup \Gamma_{ch}$. Let $I = (0, t_p)$, $t_p > 0$, let $M > 0$ be an integer, then $\triangle t = t_p/M$, $t_i = i\triangle t$, $i = 0,\ldots,M$. Let $\{\mathcal{T}_h\}$ be a regular family of finite element partitions $\mathcal{T}_h$ of $\overline{\Omega}_h$ compatible to the boundary subsets $\overline{\Gamma}_{\tau h}$, $\overline{\Gamma}_{uh}$ and $\overline{\Gamma}_{ch}$. Let $V_h \subset V$ be the finite element space of linear elements corresponding to the partition $\mathcal{T}_h$. Then $K_h = V_h \cap K$ is the set of continuous piecewise linear functions that vanish at the nodes of $\overline{\Gamma}_{uh}$ and whose normal components are non-positive at the nodes on $\cup_{s,m}\Gamma_c^{sm}$. It is evident that K_h is a nonempty, closed, convex subset of $V_h \subset V$. Let $\mathbf{u}_0 \in K_h$ be an approximation of $\mathbf{u}_0$. Further, we assume that the end points $\overline{\Gamma}_{\tau h} \cup \overline{\Gamma}_{uh}$, $\overline{\Gamma}_{uh} \cup \overline{\Gamma}_{ch}$, $\overline{\Gamma}_{\tau h} \cup \overline{\Gamma}_{ch}$ coincide with the vertices of T_{hi}. Then we have the following discrete problem:

Problem $(\mathcal{P})_h$: Find a displacement field $\mathbf{u}_h : \overline{I} \to V_h$ with

$$\mathbf{u}_h(0) = \mathbf{u}_{0h}, \tag{4.34}$$

such that for a.e. $t \in I$, $\mathbf{u}_h(t) \in K_h$ and

$$a(\mathbf{u}_h(t);\mathbf{u}_h(t),\mathbf{v}_h - \mathbf{u}_h(t)) \geq (\mathbf{f}(t),\mathbf{v}_h - \mathbf{u}_h(t)) \quad \forall \mathbf{v}_h \in K_h, \tag{4.35}$$

holds, where

$$a(\mathbf{u}_h;\mathbf{u}_h,\mathbf{v}_h) = \sum_{\iota=1}^{r} a^{\iota}(\mathbf{u}_h^{\iota};\mathbf{u}_h^{\iota},\mathbf{v}_h^{\iota}) = \int_{\Omega} c^{*}_{ijkl}(\mathbf{x},\mathbf{u}_h) e_{kl}(\mathbf{u}_h) e_{ij}(\mathbf{v}_h) d\mathbf{x},$$

$$(\mathbf{f},\mathbf{v}_h) = \sum_{\iota=1}^{r} (\mathbf{f}^{\iota},\mathbf{v}_h^{\iota}) = \int_{\Omega} F_i v_{hi} d\mathbf{x} + \int_{\Gamma_\tau} P_i v_{hi} ds. \tag{4.36}$$

To prove the existence of the discrete solution the secant modules method will be used. We reduce the initial nonlinear problem to a finite dimensional problem in the sense of the secant modules method, i.e., we transform the nonlinear problem into a sequence of linear problems, solutions of which converge to the solution of the initial problem. Then the problem leads to the solution of sequence of variational inequalities, we denote it as

Problem $(\mathcal{P})_{smh}$:

$$\mathbf{u}_h^{n+1} \in K_h, \quad a(\mathbf{u}_h^{n}(t);\mathbf{u}_h^{n+1}(t),\mathbf{v}_h - \mathbf{u}_h^{n+1}(t)) \geq (\mathbf{f}(t),\mathbf{v}_h - \mathbf{u}_h^{n+1}(t))$$
$$\forall \mathbf{v}_h \in K_h, \text{ a.e. } t \in I, \ n = 1,2,\ldots, \tag{4.37}$$

where $\mathbf{u}^n$ is the n-th approximate solution.

For simplicity let us put $\mathbf{u}_h^{n+1} \equiv \mathbf{w}_h$, $\mathbf{u}_h^{n} \equiv \bar{\mathbf{w}}_h$,.

To prove the existence of the discrete (FEM) solution $\mathbf{w}_h$ of the Problem $(\mathcal{P})_{smh}$ the technique similar to that of Nedoma, Hlaváček (2002) can be used.

From the convergence of the secant modules follows the existence of the FEM solution of the initial problem. The bilinear form $a(\mathbf{z}_h;\mathbf{w}_h,,\mathbf{v}_h) \equiv B(\mathbf{z}_h;\mathbf{w}_h,\mathbf{v}_h)$ is symmetric in $\mathbf{w}_h,\mathbf{v}_h$ and such that

$$B(\mathbf{z}_h;\mathbf{w}_h,\mathbf{w}_h) \geq c_0\|\mathbf{w}_h\|^2, \quad c_0 = \text{const.} > 0 \quad \forall \mathbf{w}_h \in V_{0h},$$
$$|B(\mathbf{z}_h;\mathbf{w}_h,\mathbf{v}_h)| \leq c_1\|\mathbf{w}_h\|\,\|\mathbf{v}_h\|, \quad c_1 = \text{const.} > 0 \quad \forall \mathbf{w}_h,\mathbf{v}_h \in V_{0h},$$

where $\|\cdot\|$ is the norm in V_{0h}. Let

$$\int_\Omega Dc^*_{ijkl}(\mathbf{w}_h,\mathbf{z}_h)e_{kl}(\mathbf{w}_h)e_{ij}(\mathbf{v}_h)d\mathbf{x}=\int_\Omega Dc^*_{ijkl}(\mathbf{w}_h,\mathbf{v}_h)e_{kl}(\mathbf{w}_h)e_{ij}(\mathbf{z}_h)d\mathbf{x}\quad\forall\mathbf{v}_h,\mathbf{w}_h,\mathbf{z}_h\in V_h$$

be the necessary condition for the construction of the Gâteaux differential of the functional (for simplicity we put $\mathcal{L}(\mathbf{v}_h,\mathbf{v}_h)=\mathcal{L}(\mathbf{v}_h)$)

$$\mathcal{L}(\mathbf{v}_h)=\frac{1}{2}\int_\Omega\int_0^1 a(\tau\mathbf{z}_h;\tau\mathbf{v}_h,\mathbf{v}_h)d\tau d\mathbf{x}$$

(see Gajewski et al. (1974)) and where we put

$$(\mathbf{f}_0,\mathbf{v}_h)\equiv(\mathbf{f},\mathbf{v}_h).$$

Then there exists the functional $\mathcal{L}$ such that

$$\begin{aligned}&B(\mathbf{w}_h;\mathbf{w}_h,\mathbf{v}_h)=D\mathcal{L}(\mathbf{w}_h,\mathbf{v}_h),\\&\tfrac{1}{2}B(\mathbf{w}_h;\mathbf{v}_h,\mathbf{v}_h)-\tfrac{1}{2}B(\mathbf{w}_h;\mathbf{w}_h,\mathbf{w}_h)-\mathcal{L}(\mathbf{v}_h)+\mathcal{L}(\mathbf{w}_h)\geq 0\ \forall\mathbf{w}_h;\mathbf{v}_h\in V_h,\end{aligned}$$

and $\mathcal{L}$ has the Gâteaux differential of second order $D^2\mathcal{L}(\mathbf{z}_h,\mathbf{w}_h,\mathbf{v}_h)$ and

$$D^2\mathcal{L}(\mathbf{z}_h,\mathbf{w}_h,\mathbf{w}_h)\geq c\|\mathbf{w}_h\|^2,\quad c=\text{const.}>0.$$

Then the functional

$$L(\mathbf{v}_h)=\mathcal{L}(\mathbf{v}_h)-(\mathbf{f}_0,\mathbf{v}_h)$$

is coercive and weakly lower semi-continuous in K_h. Moreover, the problem to find $\mathbf{w}_h\in K_h$ such that

$$D\mathcal{L}(\mathbf{w}_h,\mathbf{v}_h-\mathbf{w}_h)\geq(\mathbf{f}_0,\mathbf{v}_h-\mathbf{w}_h)\quad\forall\mathbf{v}_h\in K_h\quad\text{and fixed }\mathbf{w}_h\in K_h$$

has a unique solution.

Returning to the initial notation $\mathbf{w}_h\equiv\mathbf{u}_h^{n+1}$, then the problem (4.37) has a unique solution and

$$\lim_{r\to\infty\infty}\mathbf{u}_h^{n+1}=\mathbf{u}_h$$

in the sense of the secant-modulus method, where $\mathbf{u}_h$ is the solution of the initial problem.

Algorithm

Next, we will briefly derive the algorithm. We saw that since Problem $(\mathcal{P})_h$ is nonlinear, we applied the secant modules method, that for every $n=1,2,\dots$ it leads in the sense of this method to the solution of a sequence of discrete linear variational inequalities, above denoted as Problem $(\mathcal{P})_{smh}$. Further, for simplicity we will again use the notation $\mathbf{u}_h^{n+1}\equiv\mathbf{w}_h$, $\mathbf{u}_h^n\equiv\bar{\mathbf{w}}_h$.

The algorithm used will be based on the PDAS algorithm (see Nedoma (2005), (2010), Nedoma (2012), Nedoma et al. (2011).

Let $M>0$ be integer, then $\triangle t=t_p/M$, $t_i=i\triangle t$, $i=0,1,\dots,M$. Then

$$a(\bar{\mathbf{w}}_h,\mathbf{w}_h^{i+1},\mathbf{v}_h-\mathbf{w}_h^{i+1})\geq(\mathbf{f}(t_{i+1}),\mathbf{v}_h-\mathbf{w}_h^{i+1})\quad\forall\mathbf{v}_h\in K_h,$$

where

$$\mathbf{w}_h^i=\mathbf{w}_h(t_i),\quad\mathbf{w}_h^0=\mathbf{u}_{0h},\quad\mathbf{w}_h^{-1}=\mathbf{u}_{0h}-\triangle t\cdot\mathbf{u}_{1h}.$$

Putting $\mathbf{w}_h^{i+1}\equiv\mathbf{w}_h$, $\mathbf{w}_h^i\equiv\bar{\mathbf{w}}_h$, $\mathbf{f}(t_{i+1})\equiv\mathbf{f}_h$, then

$$a_h(\bar{\mathbf{w}}_h;\mathbf{w}_h,\mathbf{v}_h-\mathbf{w}_h)\geq(\mathbf{f}_h,\mathbf{v}_h-\mathbf{w}_h),\quad t=t_{i+1}\in I.\tag{4.38}$$

Let us define the bilinear form $A(\mathbf{u}_h,\mathbf{v}_h)$ by

$$A(\mathbf{w}_h,\mathbf{v}_h)=a_h(\bar{\mathbf{w}}_h;\mathbf{w}_h,\mathbf{v}_h).\tag{4.39}$$

Since we assumed that $\rho \geq \rho_0 > 0$, and since the bilinear form $a_h(\bar{\mathbf{w}}_h; \mathbf{w}_h, \mathbf{v}_h)$ is symmetric in $\mathbf{w}_h$ and $\mathbf{v}_h$ and satisfies $a(\bar{\mathbf{w}}_h; \mathbf{w}_h, \mathbf{w}_h) \geq c_0 \|\mathbf{w}_h\|^2_{1,N}$, $c_0 = \text{const.} > 0$, $|a(\bar{\mathbf{w}}_h; \mathbf{w}_h, \mathbf{v}_h)| \leq c_1 \|\mathbf{w}_h\|_{1,N} \|\mathbf{v}_h\|_{1,N}$, $c_1 = \text{const.} > 0$, $\mathbf{w}_h, \mathbf{v}_h \in V_h$, then the bilinear form $A(\mathbf{w}_h, \mathbf{v}_h)$ is also symmetric in $\mathbf{w}_h$ and $\mathbf{v}_h$ and

$$\begin{aligned} &A(\mathbf{w}_h, \mathbf{w}_h) \geq a_0 \|\mathbf{w}_h\|^2_{1,N}, \quad a_0^{(n)} = \text{const.} > 0, \\ &|A(\mathbf{w}_h, \mathbf{v}_h)| \leq a_1 \|\mathbf{w}_h\|_{1,N} \|\mathbf{v}_h\|_{1,N}, \quad a_1 = \text{const.} > 0, \quad \mathbf{w}_h, \mathbf{v}_h \in V_{0h}, \end{aligned} \tag{4.40}$$

hold.

Then, we have to solve in every time level the equivalent problem:

Problem $(\mathcal{P}_A)_h$: find $\mathbf{w}_h \in K_h$, such that

$$A(\mathbf{w}_h, \mathbf{v}_h - \mathbf{w}_h) \geq (\mathbf{f}_h, \mathbf{v}_h - \mathbf{w}_h), \quad \forall \mathbf{v}_h \in K_h, \quad t = t_{i+1} \in I. \tag{4.41}$$

Then Problem $(\mathcal{P}_A)_h$ is equivalent to the following problem:
find $\mathbf{w}_h \in K_h$ such that

$$L(\mathbf{w}_h) \leq L(\mathbf{v}_h), \quad \forall \mathbf{v}_h \in K_h, \quad t = t_{i+1} \in I, \tag{4.42}$$

where

$$L(\mathbf{v}_h) = \frac{1}{2} A(\mathbf{v}_h, \mathbf{v}_h) - (\mathbf{f}_h, \mathbf{v}_h).$$

We reformulate the problem as a mixed variational problem. We introduce a Lagrange multiplier space M and the trace space $W = \sqcap_{s,m} \left[H^{\frac{1}{2}}(\Gamma_c^{sm}) \right]^N = \sqcap_{s,m} H^{\frac{1}{2},N}(\Gamma_c^{sm})$, being the trace space of V_0 restricted to $\cup_{s,m} \Gamma_c^{sm}$, and its dual W'.

Let $\mathbf{w}_h, \mathbf{v}_h \in \mathbf{V}_{0h} = \left\{ \mathbf{v}_h \in H^{1,N}(\Omega) | \mathbf{v}_h = 0 \text{ on } \Gamma_{uh} \right\}$, $\boldsymbol{\mu}_{hH} = (\mu_{nh}, \boldsymbol{\mu}_{tH}) \in H^{-\frac{1}{2}}(\Gamma_c^s) \times L^{2,N-1}(\Gamma_c^s)$. We define

$$\begin{aligned} A(\mathbf{w}_h, \mathbf{v}_h) &= a_h(\bar{\mathbf{w}}_h; \mathbf{w}_h, \mathbf{v}_h), \\ (\mathbf{f}, \mathbf{v}_h) &= \int_\Omega \mathbf{F} \cdot \mathbf{v}_h d\mathbf{x} + \int_{\Gamma_\tau} \mathbf{P} \cdot \mathbf{v}_h ds, \end{aligned} \tag{4.43}$$

and

$$b(\boldsymbol{\mu}_{hH}, \mathbf{v}_h) = \langle \mu_{hn}, [\mathbf{v}_h \cdot \mathbf{n}]^s \rangle_{\cup_s \Gamma_c^s},$$

where $[\mathbf{v} \cdot \mathbf{n}]^s$, $[\mathbf{v}_t]^s$ are defined as in the previous subsection and where by $\langle \cdot, \cdot \rangle_{\Gamma_c^s}$ we denote the duality pairing between W_{hH} and $M_{hH} = M_{hn} \times M_{Ht}$, where

$$\begin{aligned} M_{hn} &= \{ \mu_{hn} \in W'_{hH}; \mu_{hn} \geq 0 \}, \\ M_{Ht} &= \left\{ \boldsymbol{\mu}_{Ht} \in L^{2,N-1}(\cup_{sm} \Gamma_c^{sm}) \,|\, \|\boldsymbol{\mu}_{Ht}\| \leq 1 \quad \text{a.e., } \boldsymbol{\mu}_{Ht} = 0 \quad \text{on } \cup_{sm} \Gamma_c^{sm} \right\}. \end{aligned}$$

Then in every time level the mixed formulation of the Signorini problem without friction consists of finding $\mathbf{w}_h \in V_h = \mathbf{u}_{2h} + V_{0h}$ and $\boldsymbol{\lambda}_{hH} = (\lambda_{hn}, \boldsymbol{\lambda}_{Ht}) \in M_{hH}$ such that

$$\begin{aligned} &A(\mathbf{w}_h, \mathbf{v}_h) + b(\boldsymbol{\lambda}_{hH}, \mathbf{v}_h) = (\mathbf{f}_h, \mathbf{v}_h) \quad \forall \mathbf{v}_h \in V_{0h}, \ t \in I, \\ &b(\boldsymbol{\mu}_{hH} - \boldsymbol{\lambda}_{hH}, \mathbf{u}_h) \leq 0 \quad \forall \boldsymbol{\mu}_{hH} \in M_{hH} = M_{hn} \times M_{Ht}, \quad t \in I. \end{aligned} \tag{4.44}$$

The existence and uniqueness of $(\boldsymbol{\lambda}_{hH}, \mathbf{w}_h)$ of this mixed variational (saddle-point) problem have been parallel as e.g. in Haslinger et al. (1996). Thus, we have

Proposition 1 *Let $-\tau_n(\mathbf{w}_h) \in M_{hn}$. Then the problem (4.44) has a unique solution $(\boldsymbol{\lambda}_{hH}, \mathbf{w}_h) \in M_{hH} \times V_h$, a.e. $t \in I$. Moreover, we have*

$$\lambda_{hn}^s = -\tau_n^s(\mathbf{w}_h),$$

where $\mathbf{w}_h$ is the solution of the primal problem.

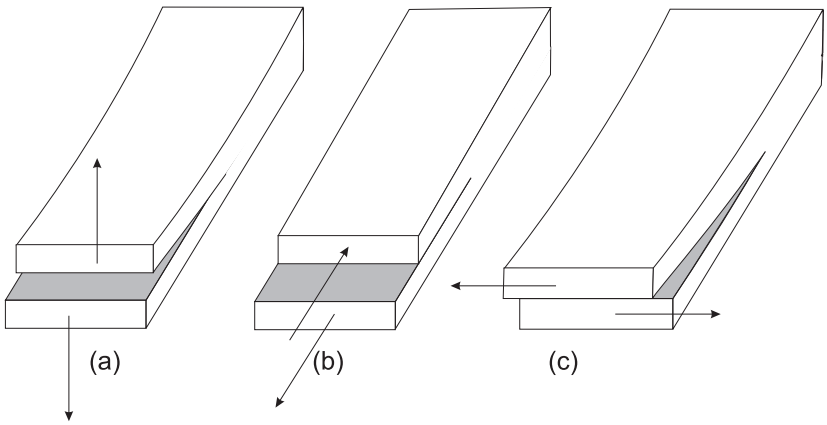

Figure 6: Fundamental modes of fracture: (a) opening mode, (b) sliding mode, (c) tearing mode.

The discussed problem is equivalent to the following problem:

Find a pair $(\boldsymbol{\lambda}_{hH}, \mathbf{w}_h) \in (M_{hn} \times M_{Ht}) \times V_h$, a.e. $t \in I$, such that
$\mathcal{H}(\mathbf{w}_h, \boldsymbol{\mu}_{hH}) \leq \mathcal{H}(\mathbf{w}_h, \boldsymbol{\lambda}_{hH}) \leq \mathcal{H}(\mathbf{v}_h, \boldsymbol{\lambda}_{hH})\ \forall (\mathbf{v}_h, \boldsymbol{\mu}_{hH}) \in V_h \times (M_{hn} \times M_{Ht})$, $t \in I$,
where

$$\mathcal{H}(\mathbf{v}_h, \boldsymbol{\mu}_{hH}) = \frac{1}{2} A(\mathbf{v}_h, \mathbf{v}_h) + b(\boldsymbol{\mu}_{hH}, \mathbf{v}_h) - (\mathbf{f}_h, \mathbf{v}_h)\,. \tag{4.45}$$

The problems (4.44) and (4.45) are equivalent to the following problem

$$\mathbf{w}_h \in K_h, \quad A(\mathbf{w}_h, \mathbf{v}_h - \mathbf{w}_h) \geq (\mathbf{f}_h, \mathbf{v}_h - \mathbf{w}_h) \quad \forall \mathbf{v}_h \in K_h,\ t \in I\,, \tag{4.46}$$

where $K_h = V_h \cap K$, $K = \{\mathbf{v} \in V, [\cdots \mathbf{v}.\mathbf{n}]^{sm} \leq 0 \text{ on } \cup_{sm} \Gamma_c^{sm}\}$.

Therefore, the algorithm PDAS from Nedoma (2005), (2010), (2012) or Nedoma et al. (2011) can be applied, where for every step of the secant modules method (i.e., for $n = 1, 2, \ldots\ldots$) the coefficients $c^*_{ijkl}(\mathbf{x}, \mathbf{u}^n_h)$, $n = 1, 2, \ldots\ldots$, must be determined as above.

5 Simulation of the jaw-bone fracture

The jaw-bones with the cysts during loading can be fractured. Thus we introduce the main ideas concerning the crack known in the theory of fracture mechanics.

5.1 Fundamentals of the fracture mechanics

From the theory of fracture mechanics it is known that there are three basic modes of crack tip displacement: (i) mode I – tensile or opening mode, (ii) mode II – in-plane shear or sliding mode, and (iii) anti-plane shear or tearing mode (see Figs 6a,b,c) and we speak about **crack tip displacement modes.**

Let us assume the Cartesian coordinates x_1, x_2, x_3, then on the plane $x_2 = 0$ we have for modes I–III:

(i) for mode I – $\tau_{11} \neq 0$, $\tau_{22} \neq \tau_{33} \neq 0$, $\tau_{12} = 0$;

(ii) for mode II – $\tau_{12} \neq 0$, $\tau_{22} \neq 0$,

(iii) for mode III – $\tau_{23} \neq 0$, $\tau_{22} = 0$, $\tau_{12} = 0$.

In Mode I the acting forces are perpendicular to the crack, pulling (stretching) the opening of a crack (Fig. 7). For the horizontal crack the forces act in the vertical direction and are of opposite signs. If both of the forces are pushing down in the crack, then the crack will start to be closed. We speak about **tensile** or **opening mode**.

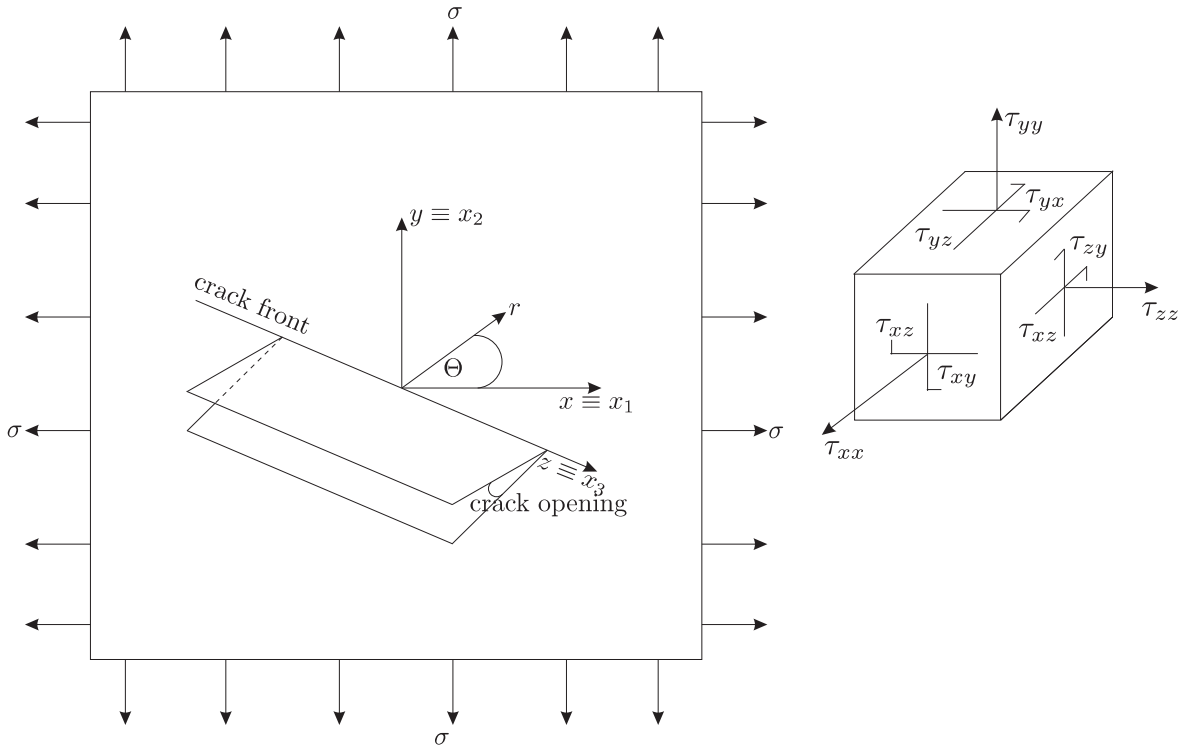

Figure 7: Opening of the crack, the Cartesian coordinate system (x_1, x_2,x_3) and the system of polar coordinates (r,Θ,z).

In Mode II the acting forces are parallel to the crack. One of them is pushing the top half of the crack back, while the other one is pulling the bottom half of the crack forward, but both along the same line. The crack is sliding along itself, i.e., acting forces create a shear crack. We speak about **in-plane shear** or **sliding mode**.

In Mode III the acting forces are perpendicular to the crack, e.g. the forces are pulling right (the bottom half of the crack) and left (the top half of the crack) and the crack is in front-back direction. We speak about **anti-plane shear** or **out-of-plane shear**. In the case if the acting forces could be pushing right and left then the same process occurs, but the forces have to be moving in opposite directions in order to grow the crack. Then we speak about **anti-plane** or **tearing mode**.

Generally, **mixed-mode type of cracks** also exist.

Next, we introduce the stress concentration factor K_T and the stress intensity factor K. The stress concentration factor K_T is introduced as the dimensionless ratio of the maximum (elastic) stress $\sigma_{\max}$ at the cut tip and the nominal applied stress σ_{nom}, that is,

$$K_T = \frac{\sigma_{\max}}{\sigma_{nom}} = 1 + 2\left(\frac{d}{r}\right)^{1/2}, \tag{5.1}$$

where d represents the cut's length and r is the radius of the cut tip (see Fig. 8).

The stress concentration factor can be found by using experimental, analytical and numerical approaches. In real bone materials the stress gradient ahead of a concentrating feature strongly grows thus the spread of plasticity is limited to a small area, which avoids plastic collapse.

Now, we introduce the stress intensity factor K for the statically loading case. The stress intensity factor K expresses the effects of the loading and geometry conditions, that is, the crack size, and its geometry.

For simplicity we will assume the 2D case. Let (x_1, x_2) be the Cartesian coordinate system with the origin at the centre of the crack of length $2a$, and let (r, Θ) be the polar coordinate system with the origin at the tip of the crack (see Fig. 9).

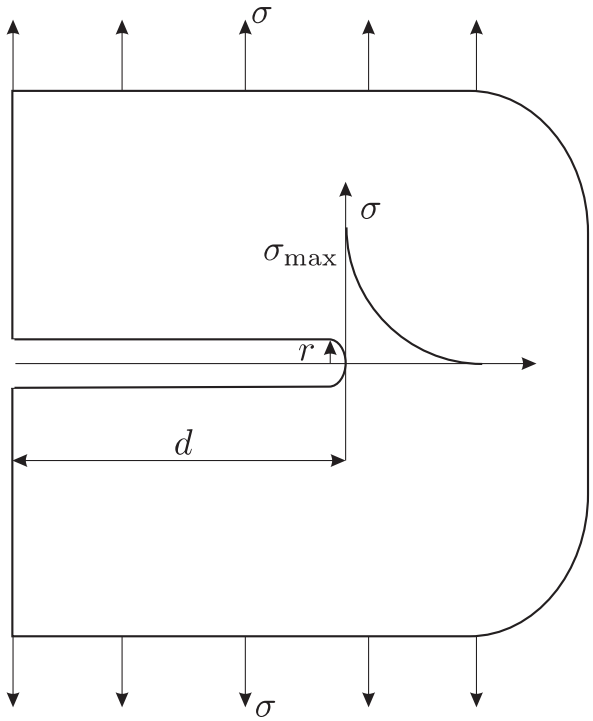

Figure 8: Stress concentration.

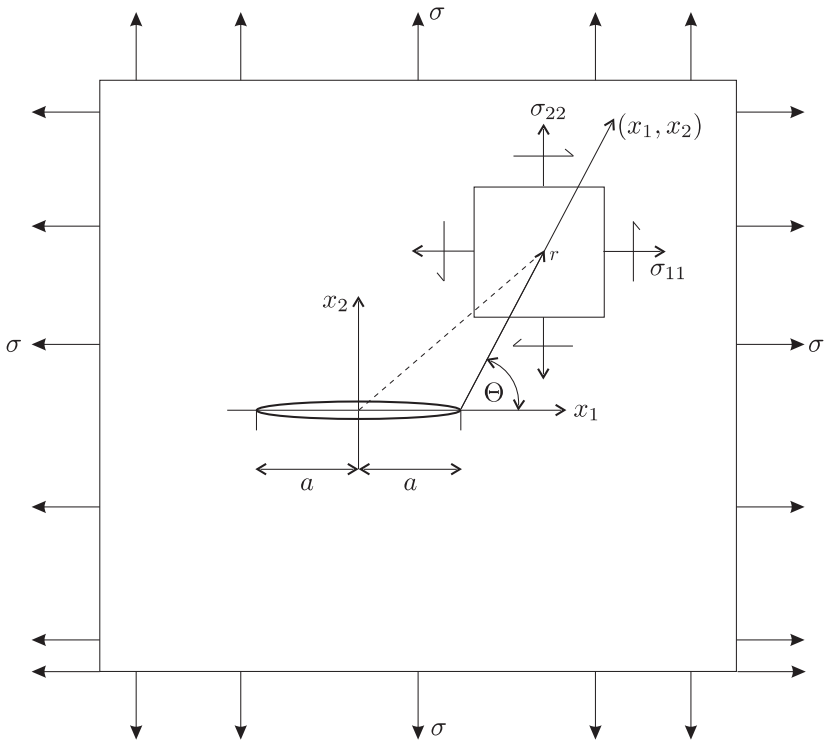

Figure 9: A crack in 2D.

The near-tip behavior of stress and displacement fields ahead a crack tip, then in the static case it can be expressed in the form

$$\sigma_{ij} = \frac{K}{\sqrt{2\pi r}}\, f_{ij}(\Theta) + O(1)\,, \tag{5.2}$$

where $O(1)$ denotes other terms which are bounded at the crack tip, and the displacement components are of the form

$$u_i = \frac{K}{2\mu}\sqrt{\frac{r}{2\pi}}\, g(\Theta), \tag{5.3}$$

where μ is the shear modulus, K denotes the stress intensity factors, where

$$K = Y\sigma\sqrt{\pi a}, \tag{5.4}$$

where Y is the geometry factor, characterizing the geometry of the crack system in relation to the applied load, $2a$ is a crack length and σ is a loading.

For the principal stresses in Mode I we find

$$\sigma_1 = \frac{K_I}{\sqrt{2\pi r}}\cos\frac{\Theta}{2}\left[1+\sin\frac{\Theta}{2}\right], \quad \sigma_2 = \frac{K_I}{\sqrt{2\pi r}}\cos\frac{\Theta}{2}\left[1-\sin\frac{\Theta}{2}\right]. \tag{5.5}$$

Since the displacements and stresses in linear elasticity are linearly proportional to the stress intensity factor, then the superposition method can also be used. Then

$$\sigma_{ij} = \frac{K_I^T}{\sqrt{2\pi r}} f_{ij}(\Theta) + \frac{K_I^B}{\sqrt{2\pi r}} f_{ij}(\Theta) + O(1) = \frac{K_I}{\sqrt{2\pi r}} f_{ij}(\Theta) + O(1)\,, \tag{5.6}$$

where $K_I = K_I^T + K_I^B$, where K_I^T is the stress intensity factor due to tension and K_I^B is the stress intensity factor due to bending. Similar results we can obtain for several load systems and for Mode II and Mode III. In general, the intensity factor K_L, $(L = I, II, III)$, for a system, which is created from m load systems, it can be found by superposition as $K_L = \sum_{i=1}^{m} K_L^i$.

The Griffith's energy concept with special reference to the stress intensity factor will illustrate crack propagation (Griffith (1920), Rice (1978a,b)). Let us consider elastic law-bones occupying the region Ω containing an internal crack of the length $2a$, with the boundary $\partial\Omega$ and loaded by a traction $\mathbf{P}$. Due to the conservation of energy law the work per unit time ($\dot{W}$), evoked by the acting loads ($\mathbf{P}$), is equal to the sum of the rates of change of the elastic strain energy ($\dot{U}_E$), plastic energy (work) ($\dot{U}_p$), kinetic energy ($\dot{U}_k$) of the bone, and the energy per unit time ($\dot{U}_L$) dissipated (lost) in the increasing area of the crack, that is,

$$\dot{W} = \dot{U}_E + \dot{U}_p + \dot{U}_k + \dot{U}_L\,, \tag{5.7}$$

where a dot denotes the differentiation with respect to time t and where $E = U_E + U_P$ is the internal energy. If the crack grows very slowly then $\dot{U}_k \equiv 0$ and also $U_k \equiv 0$. Introducing the potential energy by $\Pi = U_E - W$, and since $\frac{\partial}{\partial t} = \frac{\partial\Omega}{\partial t}\frac{\partial}{\partial\Omega} = \dot{\Omega}\frac{\partial}{\partial\Omega}$, $\Omega \geq 0$, where $\dot{\Omega}$ denotes the crack surface area growth rate per unit time, then we obtain

$$-\frac{\partial\Pi}{\partial\Omega} = \frac{\partial U_p}{\partial\Omega} + \frac{\partial U_L}{\partial\Omega}, \tag{5.8}$$

which represents that the reduction of potential energy is equal to the energy dissipated in plastic work and increasing the surface of the crack.

For the elastic jaw-bones containing a crack we introduce a crack-extension force G by

$$G = -\frac{\partial\Pi}{\partial\Omega} \tag{5.9}$$

per unit width of crack front. In the classical Griffith's theory, where an ideally brittle bone tissue are assumed, the energy dissipated in plastic deformation is small, and therefore, it can be omitted. that is,

$$G = -\frac{\partial\Pi}{\partial\Omega} = \frac{\partial U_L}{\partial\Omega} = 2\gamma\,, \tag{5.10}$$

where γ represents the energy required to form a unit of new material surface and the factor 2 means that on the right-hand side of the last equation refers to two new material surfaces formed during crack growth. This equation represents the fracture criterion for crack growth. Eq. (5.10) can be rewritten as

$$\frac{\partial(\Pi + U_L)}{\partial \Omega} = 0\,,$$

that is, the total potential energy of the system $(\Pi + U_L)$ is stationary.

Growth of the crack is considered unstable when energy of the system at equilibrium is maximum and stable when it is minimum. Then for a sufficient condition for crack stability we obtain

$$\frac{\partial^2(\Pi + U_L)}{\partial \Omega^2} \left\langle \begin{array}{ll} < 0 & \text{for a unstable fracture,} \\ > 0 & \text{for a stable fracture,} \\ = 0 & \text{for a neutral equilibrium,} \end{array} \right.$$

where the potential energy Π of the system is defined by $\Pi = U_E - W$.

External forces evoke cracks. When these external forces change in time, then after certain conditions the cracks can propagate (Fig. 10). Dynamic effects affect the stress fields near rapidly propagating cracks. A crack in a bone gives rise to a surface of discontinuity of the displacement vector. In general all components of the displacement vector retain discontinuities. Similarly as in the static case, it can be derived the stress components σ_{ij} in the neighborhood of the crack tip in a local coordinate system (Anderson (2005), Gdoutos (2005)) by

$$\sigma_{ij}(r, \Theta, t) = r^{-\frac{1}{2}} F_{ij}(\Theta, t)\,, \tag{5.11}$$

where r, Θ are polar coordinates with the centre at the crack tip, and $F_{ij}(\Theta, t)$ are functions characterizing the azimuthal dependence of the near-tip stress field and are obtained for in-plane displacements that are symmetric and antisymmetric, respectively, with respect to the plane of the crack, and for antiplane displacements. The in-plane symmetric displacements correspond to Mode I (opening mode) fracture, the in-plane antisymmetric displacements correspond to Mode II (sliding mode) fracture and antiplane displacements correspond to Mode III (tearing mode) fracture. The function F_{ij} can be expressed as the product of the stress intensity factor and a function $f_{ij}(\Theta, t)$ defining the variation with angle Θ (in time t), that is, (for derivation see Anderson (2005))

$$\sigma_{ij}(r, \Theta, t)|_{r \to 0} = \frac{K(t)}{\sqrt{2\pi r}} f_{ij}(\Theta), \quad r \to 0, K \sim O(\triangle\sigma\sqrt{2a}) \tag{5.12}$$

where $K(t)$ is the stress intensity factor that depends on the crack geometry and loading configuration, $2a$ is a crack length, $\triangle\sigma$ is the difference between the far-field stress and stress resolved on the crack walls, r is the distance to the crack tip measured from the crack exterior, $f_{ij}(\Theta, t)$ is a function characterizing the azimuthal dependence of the near-tip stress field.

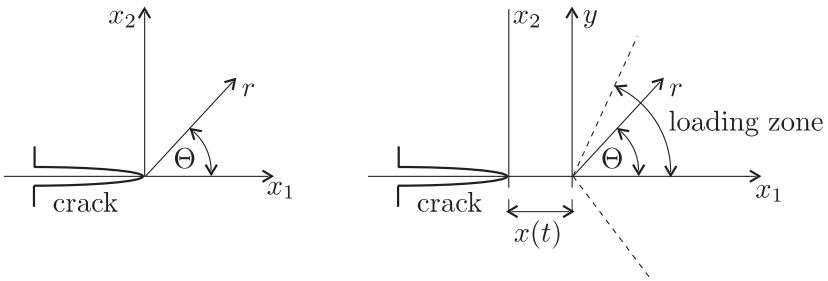

Figure 10 a,b: Propagating crack tip in 2D (a) stationary case and (b) propagating crack tips.

Next, we will introduce the near-tip behavior of the stress components for Mode I and III fractures, that is, stress components $\sigma^{\Theta}(r, \Theta, t)$ for the Mode I fracture and $\sigma^{\Theta}_{i3}(r, \Theta, t)$ for the Mode III fracture, $i = 1, 2$.

For the elastostatic case we have

$$\sigma^{\Theta} = (2\pi r)^{-\frac{1}{2}} K_I(t) f_{ij}^{I\Theta}(\Theta), \quad i,j = r,\Theta, \quad \text{for the Mode I fracture,} \tag{5.13}$$

and because $\sigma_{rr} = \sigma_{\Theta\Theta} = \sigma_{r\Theta} = 0$, we have

$$\sigma_{i3}^{\Theta} = (2\pi r)^{-\frac{1}{2}} K_{III}(t) f_{i3}^{III\Theta}(\Theta), \quad i = 1,2, \quad \text{for the Mode III fracture,} \tag{5.14}$$

where $f_{ij}^{I\Theta}(0) = f_{i3}^{III\Theta}(0) = 1$, and where the time t is a parameter, occurring due to the loading and/or due to the length of the crack if the crack propagates.

For the case of a quasi-stationary crack tip, the elastodynamic relations (5.13), (5.14) have the same form as in the elastostatic case, but the stress intensity factors are the other; we denote them as $k_I(t)$, and $k_{III}(t)$. Thus

$$\sigma^{\Theta} = (2\pi r)^{-\frac{1}{2}} k_I(t) f_{ij}^{I\Theta}(\Theta), \quad i,j = r,\Theta, \quad \text{for the Mode I fracture,} \tag{5.15}$$

and because $\sigma_{rr} = \sigma_{\Theta\Theta} = \sigma_{r\Theta} = 0$, we have

$$\sigma_{i3}^{\Theta} = (2\pi r)^{-\frac{1}{2}} k_{III}(t) f_{i3}^{III\Theta}(\Theta), \quad i = 1,2, \quad \text{for the Mode III fracture.} \tag{5.16}$$

We see that the stress intensity factors increase with time.

In the elastodynamic case of propagating crack tip (Fig. 10b), which propagates with the speed $v(t) = dx(t)/dt$, the stress intensity factors $k_I = k_I(t,v)$ and $k_{III} = k_{III}(t,v)$ are functions of the time t and the speed $v(t)$, and determination of the stress intensity factor $k_I(t,v)$ is much more complicated as in both two previous cases. Thus (Achenbach (1979))

$$\sigma^{\Theta} = (2\pi r)^{-\frac{1}{2}} k_I(t,v) f_{ij}^{I\Theta}(\Theta,v), \quad i,j = r,\Theta, \quad \text{for the Mode I fracture,} \tag{5.17}$$

and

$$\sigma_{i3}^{\Theta} = (2\pi r)^{-\frac{1}{2}} k_{III}(t,v) f_{i3}^{III\Theta}(\Theta,v), \quad i = 1,2, \quad \text{for the Mode III fracture,} \tag{5.18}$$

where $f_{ij}^{I\Theta}(0,v) = f_{ij}^{III\Theta}(0,v) = 1$. The functions $f_{ij}^{I\Theta}(\Theta,v)$ do not depend on the geometry of the crack and the loading. Its maximal value moves out of the plane of crack propagation (i.e., the plane $\Theta = 0$) because $v(t)$ increases beyond a certain value.

The crack opening displacement is thus (Achenbach (1979))

$$u^{\Theta}(t) = r^{\frac{1}{2}} U^{\Theta}(t) = \sqrt{2r}\pi^{-\frac{1}{2}} \mu^{-1} \alpha^{-1} v(t) \left(1 - v^2(t)\beta^{-2}\right) D^{-1}\left(v(t)\beta^{-1}, v(t)\alpha^{-1}\right) k_I(t,v), \tag{5.19}$$

where

$$D\left(v(t)\beta^{-1}, v(t)\alpha^{-1}\right) = \left(v^2(t)\alpha^{-2} - 2\right)^2 - 4\left(1 - v^2(t)\beta^{-2}\right)^{\frac{1}{2}} \left(1 - v^2(t)\alpha^{-2}\right)^{\frac{1}{2}}, \tag{5.20}$$

where $\alpha = \sqrt{\mu/\rho}$ is the shear wave velocity, $\beta = \sqrt{(\lambda + 2\mu)/\rho}$ is the dilatational wave velocity.

The conditions for crack tip propagation can be given by using the stress intensity factor $k_I(t,v)$ and its critical value, that is assumed to be a property of the bone tissue and it can be determined from laboratory studies. In the quasi-static linear elastic fracture mechanics we see that $K_I = K_{cI}$, representing the condition for crack instability. In the dynamic linear elastic fracture mechanics one must study initiation of the crack growth and then propagation of the crack. Therefore, the stress intensity factor for initiation of the crack growth

$$k_I(t,a,\sigma) = K_d(\dot{\sigma}), \tag{5.21}$$

where $\dot{\sigma}$ is the loading rate, t is time, a is the crack length, σ is the applied stress, and for a propagating crack

$$k_I(t,v,\sigma) = K_D(v), \quad v = \dot{a} = \frac{\partial a}{\partial t}, \tag{5.22}$$

where $K_D(v)$ represents the dynamic fracture toughness (the material bone resistance to fracture), v is the crack speed.

It is evident that, in general, the stress intensity factor k depends also on the geometry of the cracked jaw-bones, the applied loading, and the crack speed in the case of a moving (propagating) crack. Formation of a new fracture surface is accompanied by the loss of mechanical energy.

A condition for crack tip motion can be written as

$$G = G_c(v), \quad v = \dot{a}\,, \tag{5.23}$$

where $G_c(v)$ is the critical value of G, that defines the bone's resistance to fracture. It represents the energy dissipated in the fracture process accompanying crack propagation. The energy release rate per unit thickness can be written as follows

$$G = v^{-1}(\dot{W} - \dot{U}_E - \dot{U}_K)\,, \tag{5.24}$$

where a dot denotes the differentiation with respect to time t, $\dot{W}$ is the rate of work on the bone by external loads, $\dot{U}_E$ is the rate of elastic strain energy and $\dot{U}_K$ is the rate of kinetic energy. Introducing the flux of energy into the crack tip F by

$$F = \dot{W} - \dot{U}_E - \dot{U}_K\,, \tag{5.25}$$

then

$$F = Gv\,. \tag{5.26}$$

The necessary condition for fracture in the sense of the flux of energy into the crack tip is defined by

$$F = G_c(v)v\,. \tag{5.27}$$

Relation (5.26) for the Mode I fracture reduces to

$$F = -v^3\left[2\mu\alpha^2 D\left(v(t)\beta, v(t)c_s\right)\right]^{-1}\left(1 - \frac{v^2(t)}{\beta^2}\right)^{\frac{1}{2}} k_I^2(t,v)\,. \tag{5.28}$$

For slow crack tip propagation, that is, for $v \to 0$, from Eq. (5.28) it follows

$$F = \frac{1-\nu^2}{E}K_I^2(t)v\,. \tag{5.29}$$

Hence and (5.23) we find

$$K_I = K_{cI} = \left(\frac{G_c(0)E}{1-\nu^2}\right)^{\frac{1}{2}}\,, \tag{5.30}$$

where $G_c(0)$ corresponds to the quasi-static critical energy release rate, that is, K_I is equal to the toughness for fracture initiation K_{cI}.

In the non-linear elasticity or in the inelastic rheology the so-called J integral was introduced (Rice (1968a,b)). For the opening crack system (see Fig. 7) the J integral is defined by (Rice (1968a,b), Atkinson (1987), Li (1984))

$$J = \int_\Gamma \left(Wn_1 - n_i\sigma_{ij}\frac{\partial u_j}{\partial x_1}\right)ds, \quad i,j = 1,2\,, \tag{5.31}$$

where σ_{ij} and u_i are the stress and displacement components and W is the strain energy density defined by

$$W = \int_0^{e_{ij}} \sigma_{ij}de_{ij}\,, \tag{5.32}$$

where ds is the element of the arc length, $\mathbf{n} = (n_i)$ is the unit normal to the contour or path of integration Γ, which begins and ends on the crack surfaces and encloses the crack tip. For dynamic propagation, an additional term involving kinetic energy dissipation must be added.

Real polycrystalline, polyphase materials, such as bones, show more complex behavior. Due to loading on the tip of the crack a few microcracks are formed, but the system behavior remains linear.

With further rising of the loading the intensity of microcracking increases and the materials of the bone tissues in the crack tip start to be non-linear, and we speak about the nonlinear zone or the process zone. Near crack tip a few isolated microcracks and nonlinear behavior of bone tissue can be observed. Then the macrocracks start to extend and the nonlinear elastic property and the macrocrack extension occur by migration of the process zone through the material ahead of the macrocrack tip. At the crack tip the plastic behavior of bone tissues, instead of microcracking, is observed.

Fracture criteria

In the fracture mechanics when stresses at the crack tip exceed yield point, plasticity occurs. It is clear that when plasticity is minimal, then a linear elastic fracture mechanics theory can be used. The most fatal situations can occur when a crack is situated in a high-energy region, but constrained field that allows at the crack tip only small plastic deformations. The quantity of energy absorbed in plastic deformation is reduced to a minimum value and greater part of energy is used for propagation of the crack, that is, for fracture of the jaw-bones. The critical situation is described by a critical stress intensity factor K_{cL} or a critical crack-extension force G_{cL} or a critical J-integral J_{cL}, $L = I, II, III$, which may imply either a low stress acting on long crack or a small crack evoked by a high stress. Thus

$$K = K_{cL} \quad \text{or} \quad G = G_{cL} \quad \text{or} \quad J = J_{cL}, \quad \text{respectively.}$$

The left hand side corresponds to the driving force of the crack, depending on the applied loads and the geometry of the crack body. The right hand side corresponds to the material bone tissue resistance to fracture, that is, fracture toughness K_{cL}, G_{cL}, J_{cL}.

The finite element algorithm in the fracture mechanics applied to fractering of jaw-bones with cysts

Many cracks have irregular shapes, therefore, they must be studied as the three-dimensional crack models.

Let us consider a 3D cracked jaw-bones occupying the region Ω, subjected to Mode I loading. The potential energy Π of the the jaw-bones is given by

$$\Pi = \frac{1}{2}\mathbf{u}^T\mathbb{K}\mathbf{u} - \mathbf{u}^T\mathbf{F}\,, \tag{5.33}$$

where Π is the potential energy, $\mathbb{K}$ is the stiffness matrix, $\mathbf{u}$ is the displacement vector, and $\mathbf{F}$ is the global force vector. The energy release rate G is defined as the derivative of potential energy with respect to crack area, $G = -\left(\frac{d\Pi}{dA}\right)$, where A represents the crack area. In Eq. (5.33) the first term on the right-hand side is the strain energy stored in the jaw-bones and the second one is the work done by the external forces. Thus to evaluate G under fixed load for a crack of the length a, we obtain

$$G = -\left(\frac{d\Pi}{da}\right)_{load} = -\frac{\partial \mathbf{u}^T}{\partial a}[\mathbb{K}\mathbf{u} - \mathbf{F}] - \mathbf{u}^T\frac{\partial \mathbb{K}}{\partial a}\mathbf{u} + \mathbf{u}^T\frac{\partial \mathbf{F}}{\partial a}\,, \tag{5.34}$$

where the term in $[\cdot]$ brackets is zero from the definition of the finite element approximation, and in the absence of tractions on the crack face the third term on the right-hand side must vanish, because loads are constant. Thus the energy release rate for Mode I is as follows

$$G = \frac{K_I^2}{E'} = -\frac{1}{2}\mathbf{u}^T\frac{\partial \mathbb{K}}{\partial a}\mathbf{u} = -\frac{1}{2}\mathbf{u}^T\left(\sum_{i=1}^{N_c}\frac{\partial \mathbb{K}_i}{\partial a}\right)\mathbf{u}\,. \tag{5.35}$$

We see that the energy release rate is proportional to the derivative of the stiffness matrix with respect to crack length a. In Eq. (5.35) $\mathbb{K}_i$, $i = 1, \ldots, N_c$, are the elemental stiffness matrices, and N_c is the number of elements between the contours Γ_0 and Γ_1 (see Fig. 11a). Since after deformation the mesh is deformed, it would not be necessary to change all of the elements in the used mesh. It is sufficient to apply the moving mesh near the crack tip and leaving the rest of the mesh intact, and $E' = E$ for plane stress and $E' = \frac{E}{1-\nu^2}$ for plane strain for both fixed load and fixed displacement conditions, and where ν is the Poisson's ratio.

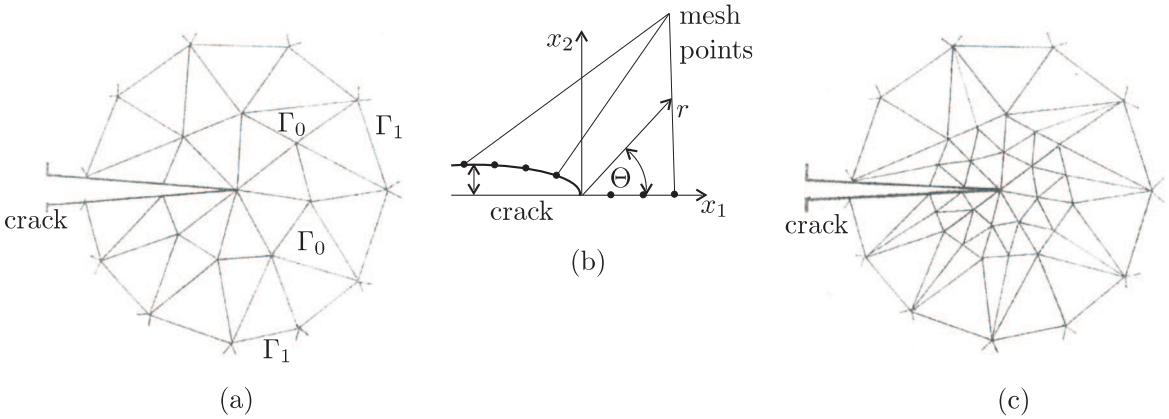

Figure 11 a,b,c: Construction of the FE mesh: (a) the mesh near the crack tip; (b) the mesh in the local coordinate system at the crack tip; (c) the design of mesh for the h-, h-p-versions of the FEM.

Numerical approaches, h- and h-p-version of finite element methods

The cracks and fractures represent the singularities in the jaw-bones occupying the domain Ω. In the neighborhood of such points, that is, in the neighborhood of the tip of cracks (Fig.11b), the exact solution is of the form

$$\mathbf{u} = \sum_{i=1}^{\infty} A_i r^{\alpha_i} f_i(\Theta), \quad \alpha_i > 0\,, \tag{5.36}$$

where $\mathbf{u}$ is the displacement vector, r and Θ are polar coordinates centered in the tip of cracks, A_i are the unknown coefficients (amplitudes), α_i are determined from the condition that the solution must satisfy the quasi-static problem and the boundary conditions on the edge of cracks. We will assume that $f_i(\Theta)$ is a smooth function, e.g., a sinusoidal vector function, so that $\alpha_1 = \frac{1}{2}$, $\alpha_2 = \frac{1}{2}$ and $A_1 = (2\pi)^{-\frac{1}{2}} k_I$, $A_2 = (2\pi)^{-\frac{1}{2}} k_{II}$, k_I and k_{II} being the Mode I or Mode II stress intensity factors, respectively. The general form of this class of functions is

$$\mathbf{u} = \mathrm{Re}\left[r^{\beta}(\log r)^{\gamma} f(\Theta)\right], \quad \mathrm{Re}|\beta| \equiv \alpha > 0, \quad \gamma \geq 0, \tag{5.37}$$

where $f(\Theta)$ is a smooth function of Θ, with the origin of polar coordinates located in the crack tip (Whiteman, Akin (1984), Nedoma (1991), (1998)).

The numerical approach is based on the construction of the design of used meshes for finite element (FEM) computations. The design of meshes is constructed by applying the mesh optimization techniques which are based on improving some aspects of the selection of a finite element method, due to the computation and the kind of desired accuracy. The addition of degree of freedom to the finite element model is an effective method how to improve the quality of the approximate solution. New degrees of freedom can be added either by subdividing selected elements into smaller ones, the so-called h-version of FEM (Fig. 11c), or by selectively increasing the order of polynomial approximation inside some elements, the so-called p-version, or by the both techniques, the so-called $h-p$-version of FEM.

The idea of a proper design of meshes is the following (see Babuška, Szabó (1981)): denote by $\mathbf{u}$ the exact solution of our studied problem, $\mathbf{u}_h$ its finite element approximation. We introduce a computable error estimator E so that $\|\mathbf{u}-\mathbf{u}_h\| \sim E$, and then an effectivity index by $\vartheta = E/\|\mathbf{u}-\mathbf{u}_h\|$. We associate to every element T_{h_i} a number η_i, the error indicator, that has to be local and can, therefore, depend only on the finite element solution $\mathbf{u}_h$ in T_{h_i} and its direct neighbors. For the energy norm we have $E^2 = \sum \eta_i^2$, where the summation goes over all elements. The estimators will be effective if $E^2 = \sum \eta_i^2$ suggests that a mesh is optimal when all error indicators are roughly equal to each other, the so-called equilibrated meshes. The equilibration principle leads immediately to the basic direction for a design of the adaptive approach. Thus, as a first step is a solution of the mesh optimization problem. That is, it is necessary to define the objective function whose minimizer is the optimal mesh. Potential energy of the finite element solution has been widely used. Since the approximate solution gives an

upper bound on the true value of the potential energy, the best mesh may be defined as the one that gives the lowest possible upper bound.

We define h-version of finite element models as a process in which the interpolating (basis) functions (polynomials of the p-th order, $p \geq 1$) are fixed for each element and the maximum diameter of the elements, denoted by $h_{\max}$, is allowed to approach zero. Further, we define the p-version of finite element models as a process in which the finite element mesh is fixed and the minimal order of basis functions (interpolating functions) p_{min}, allowed to approach infinity. The $h-p$-version of finite element models is defined as a process in which mesh refinement can be combined with increments in the order of polynomial basis functions.

The analyses of fractures by using the finite element methods were applied in practice very early (see e.g. Chan et al. (1970)).

Simulation of the mesh for fracture analyses of jaw-bones and long bones with destructive cysts

Fractures of the jaw-bones as well as the long bones and the spine, respectively, can be decomposed into four steps, that is, (i) refinement of the initially used mesh; (ii) the crack initiation; (iii) the crack opening and (iv) the crack propagation (Figs 12a,b,c). The first stage of mesh refinement can be based on the h- or $h-p$ versions of finite element methods. The stage of crack initiation, representing the beginning of the crack evolution, is crucial, but very problematic and difficult to determine the location of a crack. The fracture mechanics mostly studies the evolution of a pre-existing crack(s) or it studies the evolution of damage and a crack is initiated for a critical damage value. However, the applied codes are often unable to model the crack propagations without local collapse criterion. Some micro-failure or some inclusions in the bone can induce local stress concentrations which then can be an origin of failure(s) and crack(s) in the weakened jaw-bones. Moreover, at the crack tip a part of deformation energy is changed into the heat. But the initiations of cracks in a mesh induce severe topological changes which can be rarely supported by numerical computations. To determine locations of cracks many initiation criteria, based on critical values for mechanical state variables, stress or strain and/or rate of stress or rate of strain, respectively, are used, as well as a damage law and a critical damage parameter to localize the crack initiations can be also used. The useful crack initiation criterion can be based on a critical stress value corresponding to a characteristic properties of the jaw-bones. Then at each time step, the maximum principal stresses must be determined. If this value of principal stresses reaches the critical stress value for the jaw-bone, then a crack initiates. The algorithm then will be based on two steps: (i) firstly, an internal outline is determined in dependence to model the crack initiation and to redefine the geometry of the studied jaw-bones; (ii) secondly, the new investigated domain of jaw bones will be remeshed with dense mesh in the area of the tip of the expected crack, and with the nodes of the new outline(s) that are split to make the opening of the crack(s) possible. It means that when a crack is initiated, then we need to check, at each time step, if the crack is going to propagate, and in which direction. To determine the crack propagation the crack propagation criteria will be used and to determine the direction of the crack propagation the crack kinking criteria will be used. The mesh then will be constructed as a concentric mesh around the crack tip and coupled with singular elements to model the stress field singularity (Whiteman, Akin (1984), Barsoum (1976)). The mesh refinement around crack tip enables to obtain better information of stress-strain rates distributions in the vicinity of the crack. Since the crack tip during loading moves in time, the direction of crack propagation must be determined and then a new mesh will be constructed and refined only in the area where the crack is expected to be propagated, and moreover, with respect to time of numerical computation.

There are several methods for determination of the crack direction: the criteria will be based

(i) on stress intensity factors. That is, stress intensity factors - strength singularity at the crack tip in mode I loading - are compared with a critical value K_{Ic} of the bone tissue. Then the crack propagates when $\sqrt{2\pi r}\tau_{\Theta\Theta} = K_{Ic}$, where K_{Ic} is a critical value of the bone, r is the distance to the crack tip and $\tau_{\Theta\Theta}$ is the circumferential stress, Θ is the kinking angle (Ergodan, Sih (1963);

(ii) on energetic parameters like strain energy release rate or strain energy density (see e.g. Griffith (1920), Sih and Macdonald (1974), Hussain et al. (1974));

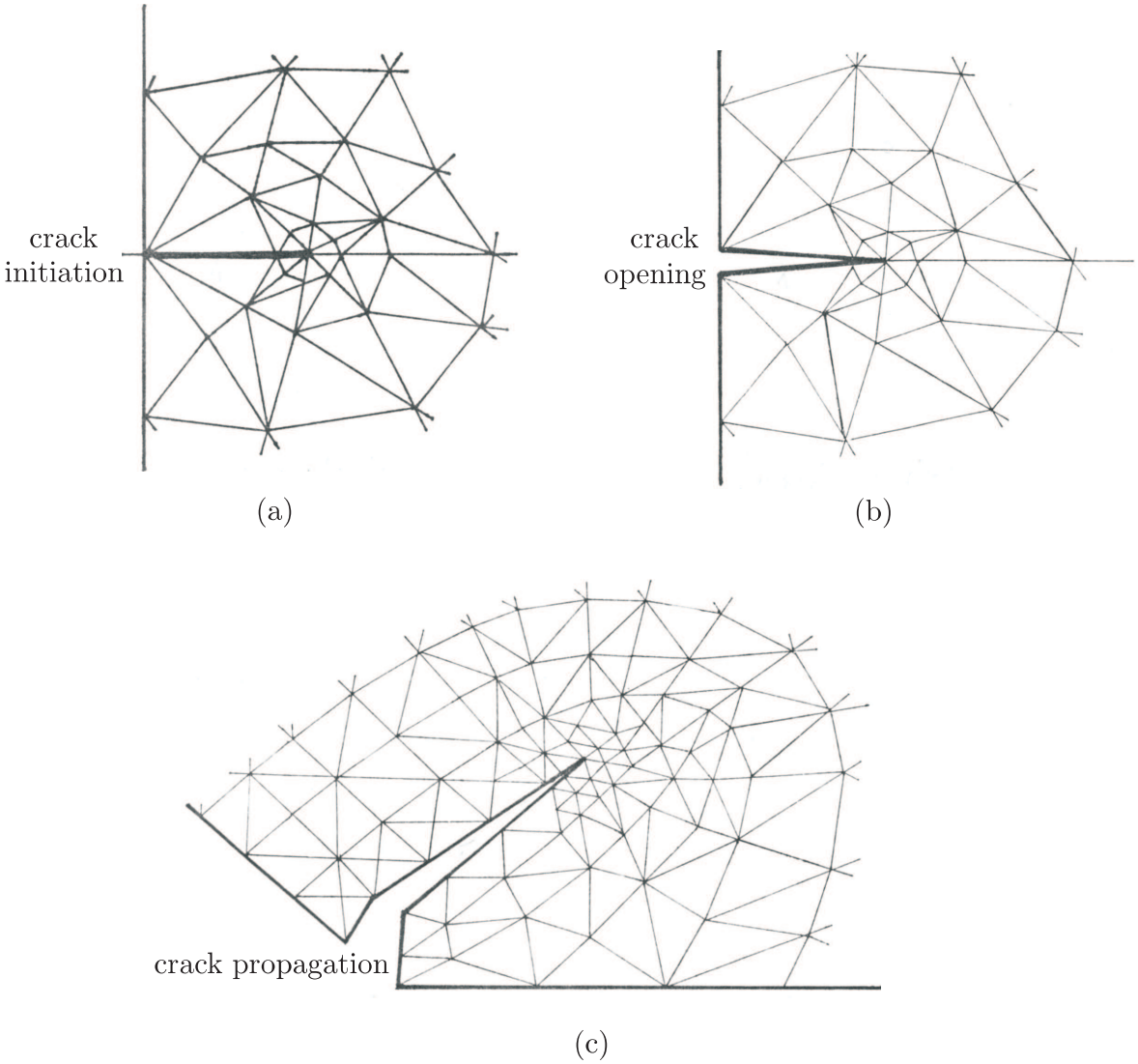

Figure 12 a,b,c: Construction of the mesh at the tip of the crack: (a) crack initiation; (b) crack opening; (c) crack propagation.

(iii) on kinking criteria. Some criteria can be based on the local fields at the crack tip, called a local approach, or based on energy distribution through the cracked part, called a global approach, like the maximal strain energy release rate criterion (see Erdogan and Sih (1963), Hussain et al. (1974);

(iv) on other criteria using a micro-void continuum damage models (see Könke (1995));

(v) on the principal stresses determined at each mesh points nearest to the crack tip.

Application of the finite element methods in fracture mechanic problems concerning analyses of fractures in the jaw-bones with cysts seems to be very useful approach.

The last technique, e.g. from the point (v), will be further discussed in more details, because it can be useful for determination of the crack(s) originated in the jaw-bones and in the long bones or in the spine, respectively.

We saw above that the osmotic pressure difference $\triangle P_0$ relates to the difference in osmolality $\triangle m$ and the temperature T, that is, $\triangle P_0 \equiv P_0^+ - P_0^- = \triangle m R_g T$, where T is an absolute temperature and R_g is the ideal gas constant. Considering the fact that the osmotic pressure will also depend

on the temperature, the problem can be also studied in the thermo-(visco-)elastic rheology or the non-linear thermo-elastic rheology, discussed above. Numerical experiments in the case of healthy hip joint deformations showed that one part of the deformation energy changed into a heat, and only a small contibution of a heat can be evoked by a friction acting on the contact boundary between the head of the femur and the acetabulum (Fig. 13). Part of a heat is then transported by the blood into greater distances from its rise. Similar situation can be also expected in the case of deformation of the jaw-bones with cysts and long bones and of the spine, respectively. The dependence of the growth of odontogenic keratocysts onto a temperature due to osmolality studies is evident, but at present determination of its magnitude is an open problem. Only mathematical simulations together with biological testing and clinical observations can clarify an effect of temperature onto a growth of the keratocysts. Experimental studies of Toller (1970b) showed that the rate of mitosis, and therefore, the osmotic processes in the case of odontogenic keratocysts are relatively quick, that is, more than one order higher than in the case of radicular cysts. Therefore, the growths of odontogenic keratocysts are several times higher than in the case of radicular cysts. Some genetic effects, like e.g. the Gorlin-Goltz syndrome, are also assumed to be a contributor to the growth of the odontogenic keratocysts.

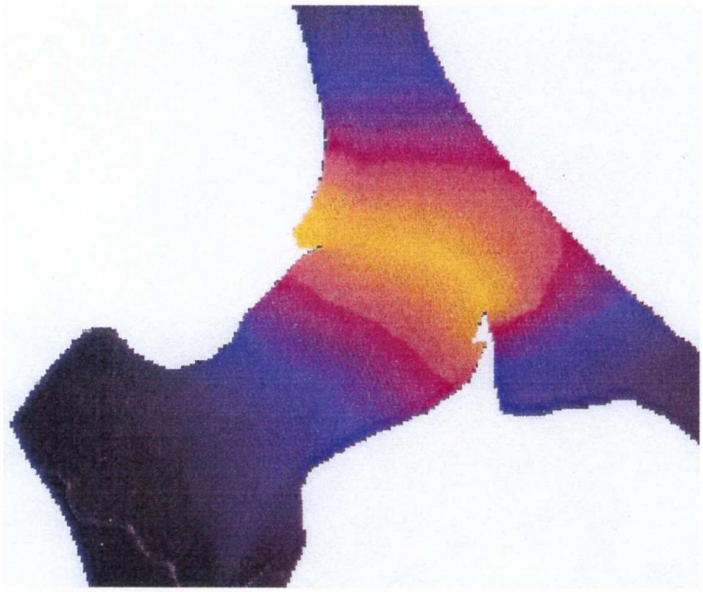

Figure 13: Propagation of heat from the contact between the femur head and the acetabulum.

The first step is a refinement of the initially introduced mesh. Firstly, we will introduce the ideas concerning a refinement of the mesh in the case of model problem in the linear thermo-elastic rheology. The generalization to the case of a mesh refinement in the nonlinear elastic rheology or thermo-visco-elastic rheology is evident.

We define h-version of finite element models as a process in which the interpolating (basis) functions (polynomials of the p-th order) are fixed for each element and the maximum diameter of the elements, denoted by $h_{\max}$, is allowed to approach zero.

Let us introduce the strain energy and the internal thermal energy by

$$2W(\mathbf{u}) = \int_\Omega c_{ijkl}(\mathbf{x}) e_{ij}(\mathbf{u}) e_{kl}(\mathbf{u}) d\mathbf{x},$$
$$2\mathcal{W}(T) = \int_\Omega \kappa_{ij}(\mathbf{x}) \frac{\partial T}{\partial x_i} \frac{\partial T}{\partial x_j} d\mathbf{x}, \tag{5.38}$$

and use the notation $2W(\mathbf{u}) = a(\mathbf{u}, \mathbf{u})$, $2\mathcal{W}(T) = a_T(T, T)$, where $a(.,.)$, $a_T(.,.)$ are the bilinear forms in the sense of the variational formulation of the investigated problem.

The strain energy $W(\mathbf{u})$ has a finite value for any $\mathbf{u} \in H^{1,N}(\Omega)$ and $(W(\mathbf{u}))^{\frac{1}{2}}$ has all of the properties of a norm, if $\mathbf{u} \in K$ and $\Gamma_u \neq \emptyset$. Further, the norm $\|\mathbf{u}\|_E^2 = (W(\mathbf{u}))$ plays an essential role

in measuring the error of finite element approximations. In fact $\|\mathbf{u}\|_E$ is equivalent to the norm $\|\mathbf{u}\|_1$, that is, there exist constants C_1, C_2 independent of $\mathbf{u}$, such that

$$C_1\|\mathbf{u}\|_1 \leq \|\mathbf{u}\|_E \leq C_2\|\mathbf{u}\|_1 \quad \text{for all } \mathbf{u} \in V\,. \tag{5.39}$$

The finite element solution $\mathbf{u}_h$ minimizes the potential energy with respect to a set of functions that can be written in the form

$$\mathbf{u} = \mathbf{w} + \sum_{i=1}^{M} c_i \boldsymbol{\varphi}_i(\mathbf{x})\,, \tag{5.40}$$

where $\boldsymbol{\varphi}_i(\mathbf{x})$ are basis functions, constructed from the element shape functions in such a way that the appropriate continuity and boundary conditions are satisfied. The basis functions depend on the choice of the finite element mesh, of the shape functions of the defined finite elements and of the mapping of the elements. The set of all functions that can be written in the form $\sum_{i=1}^{M} c_i\boldsymbol{\varphi}_i$ is called a set of finite elements and is denoted by V_h, that is, V_h is the set of all continuous vector functions in $\overline{\Omega}$, which are piecewise polynomial of the order p on the used the partition (triangulation) $\mathcal{T}_h$. We say that the domain is triangulated, if $\overline{\Omega} = \Omega \cup \partial\Omega$ is covered by a finite number of triangles T_{h_i}, forming a partition (triangulation) $\mathcal{T}_h$. Further, we define the set K_h by

$$K_h = \{\mathbf{v} \in V_h, [v_n]^{sm} \leq 0 \quad \text{on } \Gamma_c^{sm}\}\,, \tag{5.41}$$

then $K_h \subset K$ for all h, where h denotes the size of the element. The polynomial order p may vary from element to element. The number of degree of freedom, after enforcement of the Dirichlet boundary conditions, is denoted by M. Thus the finite element solution $\mathbf{u}_h$ is the function that minimize the energy functional $L(\mathbf{v})$ over the set $\mathbf{w} + K_h$.

Let $(\mathbf{u}, T)$ be the exact solution of the studied crack problem and $(\mathbf{u}_h, T_h)$ be its FE approximation, then

$$\begin{aligned}
&\frac{1}{2}\|\mathbf{u} - \mathbf{u}_h\|^2 \leq |L(\mathbf{u}) - L(\mathbf{u}_h)| \leq |W(\mathbf{u}) - W(\mathbf{u}_h)| \\
&\frac{1}{2}\|T - T_h\|^2 \leq |l(T) - l(T_h)| \leq |\mathcal{W}(T) - \mathcal{W}(T_h)|\,,
\end{aligned} \tag{5.42}$$

that is, the energy of the error of the finite element solutions are equal to or less than the error of the strain energy and/or of the internal thermal energy (for more details see Strang and Fix (1973)). Next, we will present the ideas of the adaptive algorithms only for the case of elastic part of the opening crack problem and its propagation (Nedoma (1998)).

Finite element solution minimizes the error in the energy norm (Babuška and Szabó (1981)). Therefore, the magnitude of the error in energy norm is a good measure of the overall quality of approximation. Asymptotic error estimates are useful for methods discussed. In what follows, we will assume that the points of singularity - a crack tips, are located at the nodal points.

In the h-version of a FEM method, when a sequence of meshes is obtained through uniform refinement then the asymptotic error estimate is of the form

$$\|\mathbf{u} - \mathbf{u}_h\|_E \leq C(\Omega, h, \mathcal{T}_h, p) N^{-\frac{1}{2}\min(p,a)}\,, \tag{5.43}$$

where the constant C does not depend on $\mathbf{u}$, N is the number of freedom and the absolute value of its exponent is called the rate of convergence, $\mathcal{T}_h$ is the family of triangulation (meshes), p is the polynomial degree of elements and α measures the smoothness of the exact solution. Specially, α is the smallest exponent of r in (5.36), that is, $\alpha = \alpha_1$. In a special case of equilibrated meshes, that is, optimal meshes, in which the sequence of meshes is constructed in such a way that the error associated with each element is approximately the same, the estimate leads to

$$\|\mathbf{u} - \mathbf{u}_h\|_E \leq CN^{-p/2}. \tag{5.44}$$

Here the rate of convergence is independent of α and can be made arbitrary large due to the choice of p (Nedoma (1998) and in more details in Šolín et al. (2004)).

Similar considerations are valid also in the thermal part of the studied problem in linear thermo-elastic rheology.

The second step corresponds to evolution of the crack. As it was mentioned above the determination of the crack location represents difficult problem. Micro- or macro-failures and inclusions always induce local stress concentrations which originate the failure and cracks. When a crack is localized and starts to propagate through a mesh, determination of principal stresses with high accuracy at the crack tip is of a great importance. The very usefulness technique is based on determination of the maximal principal stresses evaluated at each mesh point (integration point) nearest the crack tip. Since we determined the crack tip, then the mesh in the neighborhood of the crack tip is remeshed by a local dense mesh. Therefore, the integration points of new mesh nearest to the crack tip will be determined. Then for each of them, the eigenvalues and eigenvectors of the stress and strain tensors will be computed. The eigenvalues in these mesh (integration) points determine the magnitude of principal stresses, and/or the magnitude of principal strains, while the eigenvectors enable us to determine the principal direction of stresses (strains) and thus the direction of the crack propagation for each dense local mesh (integration) point. The resulting direction of the crack propagation will be found as a weighted average of each direction with respect to the distance between the mesh point of the dense local mesh and the crack tip. This resulting direction represent the direction of crack propagation at the recent time step of evolution of the crack. The determined direction of the maximal principal stress at the crack tip corresponds to the direction of the maximal tensile stress. The approximation used is based on the assumption that a crack propagates perpendicularly to the maximum tensile stress.

This algorithm in some cases may lead to different crack paths, that can be observed in bodies of greater dimensions. Moreover, the existence of a non-elastic (plastic) zones at the crack tips bring some of other complications. That is a reason why the other criteria, namely the energy-based criteria being based on global values of the studied loaded bodies, may be more useful in the practice. Such algorithm may be based on the strain energy, which high values tend to prevent crack growth, and therefore, the crack can grow in the direction that minimizes the strain energy.

In some cases of the jaw-bones with destructive cyst(s) situated e.g. in the ramus mandibulae (Fig. 2b) the resection technique with application of the partial TMJ prosthesis must be used (see Fig. 14). In other cases of the jaw-bones with cysts, in areas where fractures can be expected, the jaw-bones are weakened, then the above presented algorithm can be applied without any great difficulties in approximations of expected fractures.

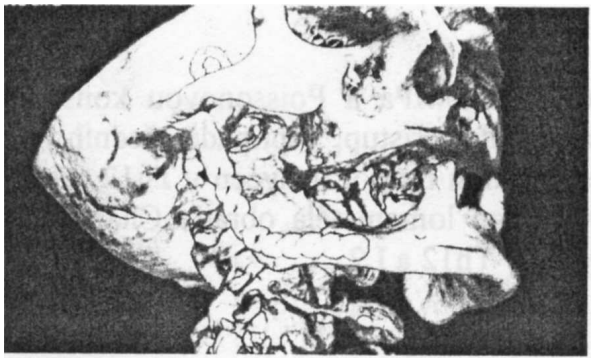

Figure 14: The bone-jaw with destructive cyst – the state after the surgical treatment.

Acknowledgement

This work was supported (partly) by the long-term strategic development financing of the Institute of Computer Science (RVO:67985807) and the Research project IGA MZCR – NT/13351-4. The author thanks to Ms. Hana Bílková for her help with typing of the paper and of preparing the figures.

Bibliography

[1] Achenbach, J. D. (1973). Dynamic effects in brittle fracture. In: Nemat-Nasser, S. Mechanics Today, vol. 1, 1–55, Pergamon Press, New York.

[2] Achenbach, J. K. (1979). Elastodynamic fracture mechanics. In: Burridge, R. (Ed.) Fracture Mechanics. Vol. XII, SIAM-AMS Proceedings, AMS, Providence, RI, NJ.

[3] Andersson, L. E. (2000). Existence result for quasistatic contact problem with Coulomb friction. Appl. Math. Optim. 42, 169–202.

[4] Anderson, T. L. (2005). Fracture Mechanics, Fundamentals and Applications. Taylor&Feancis, Boca Raton, London.

[5] Atkinson, B. H. (1987). Practice Mechanics of Rocks, Academic Press, London.

[6] Babuška, I. and Szabó, B. (1981). On the rate of convergence of the FEM. Int. J. Numer. Methods Eng. 28, 323–341.

[7] Barsoum, R. S. (1976). On the use of isoparametric finite elements in linear fracture mechanics. Int. J. Numer. Methods Engrg. 10, 25–37.

[8] Boal, D. (2002). Mechanics of the cell. Cambridge Univ. Press, Cambridge.

[9] Browne, R. M. (1975). The pathogenesis of odontogenic cysts. A review. J Oral Pathol. 4, 31–46.

[10] Browne, R. M. (1976). Some observations on the fluids of odontogenic cyst. J. Oral Pathol. 5, 74–87.

[11] Browne, R. M. (1990). Investigative Pathology of Odontogenic Cysts. CRC Press, 1st Edition.

[12] Chan, S. K., Tuba, I. S (1971). A finite element method for contact problems in solid bodies. Intern. J. Mech. Sci. 13:616–639.

[13] Chan, S. K., Tuba, I. S., Wilson, W. K. (1970). On finite element method in linear fracture mechanics. Fract. Mech. 2, 1–17.

[14] Douglas, C. W. J., Craig, C. T. (1989). Quantization of lactoferrin in odontogenic cyst fluids. J. Clin. Pathol. 42, 180–183.

[15] Eck, Ch., Jarušek, J. and Krbec, J. (2005). Unilateral Contact Problems. Variational Methods and Existence Theorems. Chapman & Hall/CRC, Taylor & Francis Group, Boca Raton, London, New York, Singapore.

[16] Ergodan, F. and Sih, G.C. (1963). On the crack extension in plane loading and transverse shear. J. Basic Engrg. 85, 519–527.

[17] Friedman. A. (1982), (2004). Variational Principles and Free Boundary Problems. Wiley-Interscience, New York.

[18] Fung, Y. C. (1965). Generalized Hooke's Law. Foundations of Solid Mechanics. Prentice-Hall, Englewood Cliffs, NJ.

[19] Fung, Y. C. (1968). Biomechanics. (Its Scope, History and Some Problems of Continuum Mechanics in Physiology). Appl. Mech. Rew., 21(1), 1–20.

[20] Fung, Y. C. (1990). Biomechanics: Motion, Flow, Stress and Growth. Springer Vlg., New York.

[21] Fung, Y. C. (1993). Biomechanics: Mechanical Properties of Living Tissues. Springer Vlg. New York.

[22] Gdontos, E. E. (2005). Fracture Mechanics. An Introduction. 2nd Ed., Springer Vlg., Dordrecht, The Netherlands.

[23] Goldman, K. E. (2009). Mandibular Cysts and Odontogenic Tumors. In: `http://emedicine.medscape.com/article/852734-print`.

[24] Griffith, A. A. (1920). The phenomena of rupture and flow in solid. Phil. Trans. Roy. Soc. London A 221, 163–197.

[25] Han, W., Jensen, G. and Shimanski, I. (1997). The Kačanov method for some nonlinear problems. Appl. Math. Numer. Math. 24, 57–79.

[26] Haslinger, J., Hlaváček, I. and Nečas, J. (1996). Numerical Methods for Unilateral Problems in Solid Mechanics (In: Handbook of Numerical Analysis, vol. IV, Elsevier, Amsterdam) pp. 313–486.

[27] Hlaváček, I. and Nedoma, J. (2002). On a Solution of a Generalized Semi-Coercive Contact Problem in Thermo-Elasticity, Math. Comput. Simulat. **60,** pp. 1–17.

[28] Hussain, M. A., Pu, S. L. and Underwood, J. H. (1974). Strain energy release rate for a crack under combined Mode I and Mode II. Fract. Analysis, ASTM STP 560, Philadelphia, 2-28.

[29] Killey, H. C., Kay, L. W., Sir Bradlaw, R. (1966). Benign cystic lesions of the jaws. Edinburgh and London.

[30] Könke, C. (1995). Damage evolution in ductile materials: from micro- to macro-damage. Comp. Mech. 15, 495–510.

[31] Larsen, P. E., Hegtvedt, A. K. (1998). Chapter 78, Odontogenesis and Odontogenic Cysts and Tumors. In: Cummings, C.W. et al. (1998). Otolaryngology-Head and Neck Surgery, 3rd Ed., Mosby, St. Louis.

[32] Li, V. C. (1984). The finite element method by employing the singular elements with concordant displacement at the crack tip. Eng. Fract. Mech., 19, 959–972.

[33] Magar, V., Ward, J., Franks, S., Landini, G. (2002). A model on the dynamics of odontogenic cyst growth. Report on a problem studied at the UK Mathematics-in-Medicine Study Group Nottingham 2002. `http://www.maths-in-medicine.org/uk/2002/dental-cysts/`.

[34] Malassez, L. (1885). Sur Le role des debris epitheliaux papdentaires. Arch. Physiol. Norm. Pathol. 5, 309–340; 6, 379-449.

[35] Murray, J. D. (2003). Mathematical Biology, 3rd Edition, Springer Vlg. Berlin.

[36] Nedoma, J. (1983). On one Type of Signorini Problem without Friction in Linear Thermo-Elasticity, Appl. Math. **28** 6, 393–407.

[37] Nedoma. J. (1987). On the Signorini Problem with Friction in Linear Thermo-Elasticity: the Quasi-Coupled 2D-Case, Appl. Math. **32** 3, 186–199.

[38] Nedoma, J. (1991). Static stress-strain analysis of human joint and their artificial substitutes. TR V-516,ICS AS CR, Prague.

[39] Nedoma, J. (1993). Mathematical Modelling in Biomechanics. Bone- and Vascular-Implant Systems. Habilit. Thesis. ICS AS CR, Prague.

[40] Nedoma, J. (1998). Numerical Modelling in Applied Geodynamics, John Wiley&Sons, Chichester.

[41] Nedoma, J. (2005). Mathematical models of artificial total replacements of joints. I. Dynamical loading of THA and TKR. Mathematical 2D and 3D models. TR 950, ICS AS CR, Prague (in Czech).

[42] Nedoma, J. (2010). Special Problems in Landslide Modelling. Mathematical and Computational Methods. In: Werner, E.D., Friedmann, H.P. (2010). Landslides: Causes, Types and Effects. Nova Sci. Publ., New York, 263-386.

[43] Nedoma, J. (2012). Mathermatical modelling of some consequences of hurricanes: The proposal of research project, mathematical and computational methods. In: Tarasov, A. and Demidov, M. (2012). Eddies and Hurricanes: Formation, Triggers and Impact. Nova Sci. Publ., New York (in print).

[44] Nedoma, J. Hlaváček, I. (2002). Solution of a semi-coercive contact problem in a non-linear thermo-elastic rheology. Math. Comput. Simul. 60, 119-127.

[45] Nedoma, J., Bartoš, M., Kestřánek sen., Z., Kestřánek jr., Z. and Stehlík, J. (1999). Numerical Methods for Constrained Optimization in 2D and 3D Biomechanics, Numer. Linear Algebra Appl. **6,** 557-586.

[46] Nedoma, J. et al. (2006). Biomechanics of Human Skeleton and Artificial Replacements of Its Parts. EUROMISE - Charles University, Karolinum Press, Prague (in Czech).

[47] Nedoma, J. et al. (2011). Mathematical and Computational Methods in Biomechanics of Human Skeletal Systems. An Introduction. John Wiley&Sons, Hoboken, New Jersey.

[48] Norton, N.S. (2007). Netter's Head and Neck Anatomy for Dentristy. Saunders, Elsevier, Philadelphia, Pa.

[49] Rice, J.R. (1968a). Mathematical Analysis in the Mechanics of Fracture. Chapter3. In: Liebowitz, H. (Ed.). Fracture, An Advanced Treatise, Vol. 2, Academic Press, New York, 191-331.

[50] Rice, J.R. (1968b). A Path-Independent Integral and the Approximate Analysis of Strain Concentration by Notches and Cracks. J. Appl. Mech., 35, 379-386.

[51] Rice, J.R. (1978a). Thermodynamics of the Quasi-static Growth of Griffitth Cracks. J. Mech. Phys. Solids, 26, 61-78.

[52] Rice, J.R. (1978b). Elastic-plastic fracture mechanics. In: Erdogan, F. (Ed.). The Mechanics of Fracture, AMD, 19, 23-53.

[53] Shaefer, W.G., Hine, M.K. and Levy, B.M. (1983). A Textbook of Oral Pathology. W.B. Saunders Co, 4th Edition, 258-317.

[54] Shear, M. (1992). Cysts of the Oral Regions. Wright, Oxford, 3rd Edition.

[55] Shear, M. (1994). Developmental odontogenic cysts. An update. J. Oral. Pathol. Med. 23, 1-11.

[56] Shear, M., Speight, P.M. (2007). Cysts of the Oral and Maxillofacial Regions. Blackwell Publ., 4th Edition, ISBN: 978-14051-4937-2.

[57] Sih, G.C. (1973). Handbook of Stress Intensity Factors for Researches and Engineers. Inst. of Fracture and Solid Mechanics, Lehigh University, USA.

[58] Sih, G.C. and Macdonald, B. (1974). Fracture mechanics applied to engineering problems - strain energy density fracture criterion. Engrg. Fract. Mech. 6, 361-386.

[59] Smith, A.J., Smith, G., Browne, R.M. (1983). Protein differences in odontogenic cyst fluids. IRCS Med. Sci. 11, 117-

[60] Smith, A.J., Smith, G., Browne, R.M. (1986). Analysis of odontogenic cyst fluid aspirates. IRCS Med. Sci. 14, 304-

[61] Smith, A.J., Mathews, J.B., Mason, G.I. and Browne, R.M. (1988). Lectoferrin in aspirates of odontogenic cyst fluid. J. Clin. Pathol. 41, 1117-1119.

[62] Soames, J.V., Southam, J.C. (1998) Oral Pathology. Oxford Univ. Press, 2nd Edition, Oxford.

[63] Strang, G. and Fix, G.J. (1973). An Analysis of the Finite Element Method. Prentice-Hall, Englewood Cliffs, NJ.

[64] Stranz, M. and Kastango, E.S. (2002). A review of pH and osmolarity. International Journal of Pharmaceutical Compounding, vol. 6, no 3, May/June 2002, 216-220.

[65] Šolín, P., Segeth, K., and Doležal, I. (2004). Higher-Order Finite Element Methods. Chapman&Hall/CRC, Boca Raton, FL.

[66] Thieme, H.R. (2003). Mathematics in Population Biology. Princeton Univ. Press.

[67] Toller, P.A. (1966). Permeability of cyst walls in vivo: Investigations with radioactive tracers. Proc. of the Royal Society of Medicine 59, 724-729.

[68] Toller, P.A. (1970a). Protein substances in odontogenic cyst fluids. Br. Dent. J. 128, 317-322.

[69] Toller, P.A. (1970b). The osmolarity of fluids from cysts of the jaws. Br. Dent. J. 129, 275-278.

[70] Tombs, M.P., Peacocke, A.R. (1974). The Osmotic Pressure of Biological Macromolecules. Clarendon Press, Oxford.

[71] Underbrink, M. and Pou, A. (2002). Odontogenic Cysts and Tumors. Grand Round Presentation, UTMB, Dept. of Otolaryngology.

[72] Ward, J.P., Magar, V., Franks, S.J. and Landini, G. (2004a). A mathematical model of the dynamics of odontogenic cyst growth. Analytical and Quantitative Cytology and Histology 26 (1), 39-46.

[73] Ward, J.P., Magar, V., Franks, S.J. and Landini, G. (2004b). A model on the dynamics of odontogenic cyst growth. Manuscript.

[74] Whiteman, J.R. and Akin, J.E. (1984). Finite elements, singularities and fracture. The Mathematics of Finite Elements and Applications III. In: J.R. Whiteman (Ed.), Academic Press, London, 35-51.

[75] Zeidler, E. (1990a,b). Applied Functional Analysis: Application to Mathematical Physics, vol. 108-109, Springer Vlg., New York.